Profiling of synaptic transcriptome

Dissertation zur Erlangung des akademischen Grades

Doktor der Naturwissenschaften
(Dr. rer. nat.)

eingereicht am Fachbereich Biologie Chemie Pharmazie

der Freien Universität Berlin

vorgelegt von

Ana Babic

aus Virovitica, Croatia

Berlin 2014

Die vorliegende Arbeit wurde von Januar 2010 bis August 2014 am

Max-Delbrück-Centrum für Molekulare Medizin

unter der Anleitung von

Dr. Wei Chen

angefertigt.

1. Gutachter: Dr. Wei Chen

2. Gutachter: Prof. Dr. Constance Scharff

Disputation am 18. Juni 2015

Abstract

Unique neuronal morphology and the information processing that occurs in distal dendritic and axonal compartments necessitates the cellular mechanisms for synthesis, modification, delivery and degradation of dendritic and synaptic proteins locally. In recent years, a variety of individual RNA molecules, regulating protein translation and other cellular functions, have been discovered in neuronal compartments . However, it is not fully understood which of the coding and noncoding genes are expressed in neuronal compartments and which function they might have in mRNA localization and RNA-regulated translation. To address this, we characterized the gene expression profile of mouse neuronal processes using a combination of synaptosomes isolation with high-throughput sequencing. We identified 19,303 protein coding genes expressed in mouse hippocampal synaptosomes. Of these, 1,446 were enriched by more than two fold compared to adult mouse hippocampus, including genes with previously described synaptic functions. Notably, by taking such an unbiased approach, we identified mRNAs expected to be entirely somatic, among them transcription factors, enriched in synaptosomes. The localization pattern of a subset could be validated by high resolution *in situ* hybridization.

Among different classes of non-coding RNAs, circular RNAs (cRNAs), formed by the atypical head-to-tail splicing of exons, have re-emerged as a potentially interesting RNA species. We profiled the expression of cRNAs in different mouse tissues and found them to be more abundant in the brain. Interestingly, the loci deriving cRNAs in the brain showed enrichment of genes with synapse-related functions. More intriguingly, on average, cRNAs were more abundant in synaptosomes compared to the whole brain homogenate. All these observations suggest synapse related function of cRNAs in brain. Consistently with this hypothesis, we could observe the change of cRNAs expression during synaptogenesis in mouse hippocampus, some of which are

not accompanied with the expression changes of their linear hosts. Moreover, we could demonstrate the expression change of a dozen of circular RNAs upon neuronal stimulation. Finally, we identified protein interaction partners of an abundant circular Homer1 transcript, many of which are known components of neuronal RNA transport granule, suggesting the circular RNAs might be actively transported to distal parts of the neuron.

In conclusion, in this study, using an unbiased approach, we have characterized distally localized neuronal transcriptome, including both coding and non-coding RNAs. Our data serves an important resources for further functional study of RNA localization and local regulation in neuron.

Zusammenfassung

Die einzigartige Morphologie von Neuronen und der Informationsfluss, der in dendritischen und axonalen Kompartimenten stattfindet, erfordern einen zellulären Mechanismus für die Regulation von Synthese, Modifikation sowie die Zufuhr und den Abbau von dendritischen und synaptischen Proteinen. Kürzlich wurde eine Vielzahl von verschiedenen RNA Mokelülen detektiert, welche die Proteinsynthese sowie andere zelluläre Funktionen in neuronalen Kompartimenten regulieren. Es ist jedoch unklar, welche kodierenden und nicht-kodierenden Gene in neuronalen Kompartimenten exprimiert sind und welche Rolle diese in Prozessen wie mRNA Lokalisation und RNA-regulierter Translation spielen. Um diese Fragestellung anzugehen, haben wir mittels Synaptosomen-Präparation und Hochdurchsatzsequenzierung das Genexpressionsprofil von neuronalen Fortsätzen charakterisiert. Wir identifizierten 19 303 protein-kodierende Gene in Synaptosomen des Hippokampus der Maus. Mehr als 1 446 waren zweifach angereichert im Vergleich zu Homogenaten des gesamten Gehirnes; unter ihnen Gene mit bereits beschriebenen synaptischen Funktionen. Bemerkenswerterweise haben wir mittels dieses unvoreingenommenen Ansatzes auch Transkriptionsfaktoren identifiziert, die in Synaptosomen angereichert sind. Das Lokalisationsmuster einiger ausgewählter Kandidaten konnte mit Hilfe hochauflösender *in situ* Hybridisierung validiert werden.
Zirkuläre RNAs (cRNAs), die durch nicht-konventionelles “head-to-tail” Splicing von Exons generiert werden, sind kürzlich erneut als eine potentiell interessante Klasse von regulatorischen RNAs (neben weiteren nicht-kodierenden RNAs) in den Fokus gerückt. Wir haben die Expression von cRNAs in unterschiedlichen Geweben des Maus untersucht und zeigen, dass diese im Gehirn am stärksten exprimiert sind. Interessanterweise waren die Genorte, welche die Expression von cRNAs steuern, häufig mit synaptischen Funktionen verknüpft. Ferner waren cRNAs im Durchschnitt

stärker in Synaptosomen, als in Ganzhirnhomogenaten angereichert. Diese Beobachtungen deuten auf eine Funktion verbunden mit Synapsen im Gehirn hin. Im Einklang mit dieser Hypothese konnten wir eine Veränderung der Expression einiger cRNAs während der Synaptogenese im Hippokampus der Maus feststellen. Einige Veränderungen der cRNA Expression waren unabhängig von der Expression ihrer linearen Hostgene. Desweiteren konnten wir zeigen, dass einige cRNAs ihre Expression nach neuronaler Stimulierung ändern. Zum Schluss haben wir Proteininteraktionspartner einer stark angereicherten cRNA des Homer1 Transkriptes identifiziert. Darunter sind viele bekannte Komponenten von neuronalen RNA Transportgranula. Dies deutet darauf hin, dass cRNAs aktiv zu distalen Bereichen der Neuronen transportiert werden können.

Zusammenfassend haben wir mittels eines unvoreingenommenen Ansatzes das distal lokalisierte neuronale Transkriptom, bestehend aus kodierenden- als auch nicht-kodieren RNAs, charakterisiert. Unsere Daten dienen als wichtige Informationsquelle für weitere funktionelle Studien der RNA Lokalisation sowie der regulatorischen Prozesse, die lokal in Neuronen stattfinden.

TABLE OF CONTENTS

ACKNOWLEDGEMENTS

PhD has been an exciting and invaluably instructive part of my life. For this, I am indebted and thankful to many people. First of all I would like to acknowledge my supervisor Wei Chen, for giving me the opportunity to work in his lab and for his support during my PhD.

I am grateful to Xintian You (Arthur) for fruitful discussions and immense help all these years.

I am obliged to the whole Wei Chen lab; Claudia Quedenau, Hang Du, Martina Weigt, Jingyi Hou, Wei Sun (Sunny), Claudia Langnick, Madlen Sohn, Mirjam Feldkamp, Yuhui Hu, Sebastian Froehler, Tao Chen, Qingsong Gao, as well as our former members Yongbo Wang, Na Li and Wei Sun, for their help, discussions and the nice time we had together.

For the project “Characterization of circular RNAs in the brain” I would like to thank Prof. Erin Schuman and all members of her lab at Max Planck Institute for Brain Research, Frankfurt am Main, especially Irina for helping me with the “Zusammenfassung” and Tristan for introducing me to high resolution *in situ* technology.

I would like to thank Stefanie Weinert for introducing me to good scientific practice and invaluable help in synaptosomes isolation experiments.

I am grateful to Prof. Dr. Constance Scharff for kindly being my external supervisor in Free University of Berlin and for critically reviewing my thesis.

I would like to acknowledge the staff of Berlin Institute for Medical Systems Biology (BIMSB); especially Jennifer and Sabrina for the support with the bureaucracy and paper work. I would also like to acknowledge our collaborators at MDC; the laboratory of Stefan Kempa for their contribution in proteomics.

The family that I chose for myself is immense. No names have to be written on the paper for they are written in my heart. I would like to express my gratitude to Nick, Andranik and Bojan for being always there to listen to me, cheer me up and believing in me, as well as Toshiaki and Marlon for their generous help through the first half of my PhD. Your supports have always been so important.

Finally, I would like to thank my family; my parents Ivica and Katarina, my brother Hrvoje and my sister Iva, for their great support and love.

STATEMENT OF CONTRIBUTION

The project was conceived and supervised by Wei Chen.

The work that led to this thesis was a collaborative project between the group of Wei Chen at MDC Berlin and group of Erin Schuman at Max Planck for Brain Research, Frankfurt am Main.

Experiments were designed by Wei Chen, myself and Xintian You. Most of the experiments were performed by myself with the help of Claudia Quedenau.

Xintian You designed and performed all the computational analyses presented here.

All other figures except for the ones mentioned below were generated by myself.

Figure 1- 8 were adapted from publications with permission from publisher.

Figure 10B and 10C were produced by Stefanie Weinert.

Figure 15 and Figure 21C were produced by Tristan Will.

LC-MS/MS measurements were performed by Guido Mastrobuoni within the collaboration with the laboratory of Stefan Kempa.

1. INTRODUCTION

1.1 Gene expression regulation

Every organism owns a genome that stores the information necessary to build and maintain a living system. The information stored in the genome is released through the coordinated activity of enzymes and other proteins in a complex series of biochemical reactions referred to as gene expression. Dynamic regulation of gene expression gives rise to different cellular phenotypes enabling organisms to accommodate metabolic demands, maintain homeostasis and capacity to grow in response to the environmental change (Brown TA, 2002).

The long accepted paradigm of normal flow of biological information from DNA to RNA to protein (Crick, 1970) has been constantly expanded throughout last four decades, in particular by recent advances in genome research (Shapiro, 2009). New insights about the complexity and flexibility of genome have changed our understanding of the architecture, activity and regulation of the eukaryotic genome (Qureshi et al. 2012). Genome-wide analyses of the eukaryotic transcriptome have revealed that the majority of the genome is transcribed, producing large numbers of non-protein-coding RNAs (ncRNAs) which have myriad of regulatory and other functions. Transcriptional complexity is further enhanced by alternative splicing (Kornblihtt et al., 2013), alternative polyadenylation (Giammartino et al., 2011), as well as from alternative promoter and enhancer elements (Pal et al., 2011) giving rise to messenger RNAs encoding proteins that are processed from primary transcripts into multiple transcript isoforms. Nowadays, with gene expression being recognised as a highly interconnected multistep process including transcription, splicing, export, stability, localization and translation (Hawkins et al., 2010), the challenge is to uncover both the molecular details of each single step as well as the mechanisms of

coordination among them in order to fully understand the regulation of gene expression.

1.1.1 Transcriptional regulation of gene expression

Transcriptional regulation is the first node in controlling the generation of functional gene products whose biological information is required by the cell at a particular time. Transcriptional process is driven by regulatory elements present on the DNA together with many different trans-acting factors (transcription factors, chromatin remodelers, polymerases, helicases, kinases, topoisomerase, proteases etc.) that are forming mega dalton complexes which assemble and disassemble from DNA in seconds (Coulon et al. 2012). Thanks to the development of suitable high-throughput technologies, such as microarray and novel sequencing technology, big advances have been made in the last decade to understand the molecular mechanisms underlying transcriptional regulation. In particular, a good fraction of ENCODE project (the Encyclopedia of DNA Elements) was devoted to map all regions of transcription, transcription factor association, chromatin structure and histone modification in the human genome sequence resulting in functional biochemical annotation for 80% of the components of the human genome (The ENCODE Project Consortium, 2012).

1.1.2. Post-transcriptional regulation of gene expression

Post-transcriptional regulation in eukaryotic organisms includes all the mechanisms of gene expression control that are employed after transcription has been initiated. After transcription, pre-mRNAs undergo nuclear processing including 5' capping, 3' polyadenylation, pre-mRNA splicing and in some cases RNA editing. Together with further mechanisms of post-transcriptional regulation such as mRNA transport, RNA quality-control, storage and degradation mechanisms, providing cells with an extended option to fine−tune their proteomes. Finally, it is the concentration of mature mRNA in the cytoplasm that regulates how much protein will be produced, with each step of this interlinked process regulated in an mRNA-specific and context dependent manner (Moore, 2005). Unique combination of protein factors and regulatory RNAs binding along the mRNA transcripts, constitutes a messenger ribonucleoprotein particle (mRNP) which decides what happens with mRNA in the cytoplasm, by regulating subcellular localization, translation and decay. To meet the demands of complex organism development and to provide appropriate response to environmental stimuli, each step of these processes needs to be finely regulated with deregulation potentially resulting in pathological conditions.

Recent studies underscored the predominance and complexity of post-transcriptional regulation by showing that about ~60% of the variation in the protein abundance can not be explained by measuring mRNAs alone (Schwanhausser et al., 2011, Vogel et al., 2012). The post-transcriptional regulatory mechanisms, such as microRNAs (Ameres et al., 2013) and the RNA-binding proteins (RBPs) that bind and presumably co-regulate sets of functionally related transcripts (Keene, 2007), determine the protein concentrations to a similar extent as transcriptional regulation does. However, by large, the contribution of individual modes of post-transcriptional regulation to

control cellular protein abundances in different physiological contexts is not known. The two modes of post-transcriptional control that gained attention only recently are subcellular RNA localization and local translation, providing a mechanism for regulating gene expression in spatial dimension and enabling restriction of gene expression to specific sites within a cell.

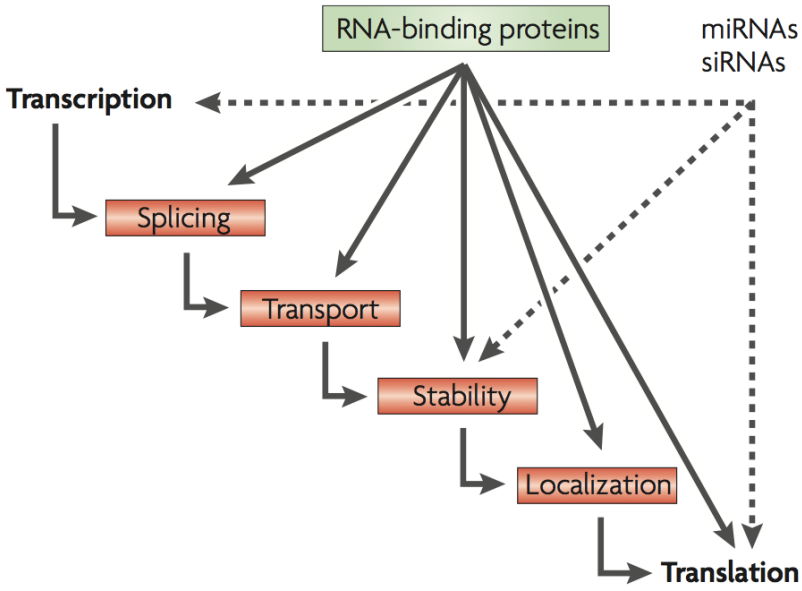

Figure 1. Post-transcriptional regulation of gene expression in eukaryotes involves several coordinated steps of regulation between transcription and translation. RNA-binding proteins and non-coding regulatory RNAs direct the splicing, export, stability, localization and translation outcomes for multilple RNAs simultaneously. Adapted by permission from Macmillan Publishers Ltd: Nature Reviewes Genetics, Keene JD, RNA regulons: coordination of post-transcriptional events, Vol.8 (7)), pp 533-543, copyright (2007).

1.1.3. Spatio-temporal regulation of gene expression

Messenger RNA localization coupled with regulated translation was initially thought to be used only by a handful of transcripts in order to restrict the protein synthesis to specialized compartments of polarized and asymmetric cells, as early embryo and neuronal cells. Yet recent systems-level analyses in different model systems showed that more than half of the transcripts are localized within distinct subcellular compartments (Cajigs et al., 2012, Lecuyer et al., 2007) suggesting that the locally regulated translation is a more general phenomenon used to control gene expression. In the study of mRNA localisation dynamics in Drosophila embryogenesis, 71% of 3370 genes analysed were shown to encode subcellularly localized mRNAs (Lecuyer et al., 2007) while in neurons, recent study revealed a large number of mRNA residing in dendrites and axons, contrary to the previous belief that local synthesis might be used only in special cases during some forms of plasticity (Cajigas et al., 2012). Moreover, numerous studies in a range of model organisms and cell types also showed that key components of the mRNA localization machinery are conserved from yeast to mammals (reviewed in Quattrone et al., 2012).

There are several advantages arising from localization of mRNA instead of proteins. Firstly, by restricting gene expression to specific subcellular domains in the cytoplasm, mRNA localization also enhances a temporal regulation of gene expression. It would take much longer if specific signal received in cell periphery would first have to be delivered to the nucleus where transcription would start followed by other RNA processing and translation steps before the protein would finally reach the site of stimulation. Secondly, transporting proteins is more costly than localisation of one transcript to a distinct site, which then can be translated multiple times, since in general in mammalian cells mRNAs are produced at a much

lower rate than proteins are, with on average two copies of a given mRNA per hour, while dozens of copies of the corresponding protein are produced per hour. Lastly, producing proteins locally contributes to an accumulation of proteins at discrete sites, which together with selective organelle targeting establishes cell polarity and complexity.

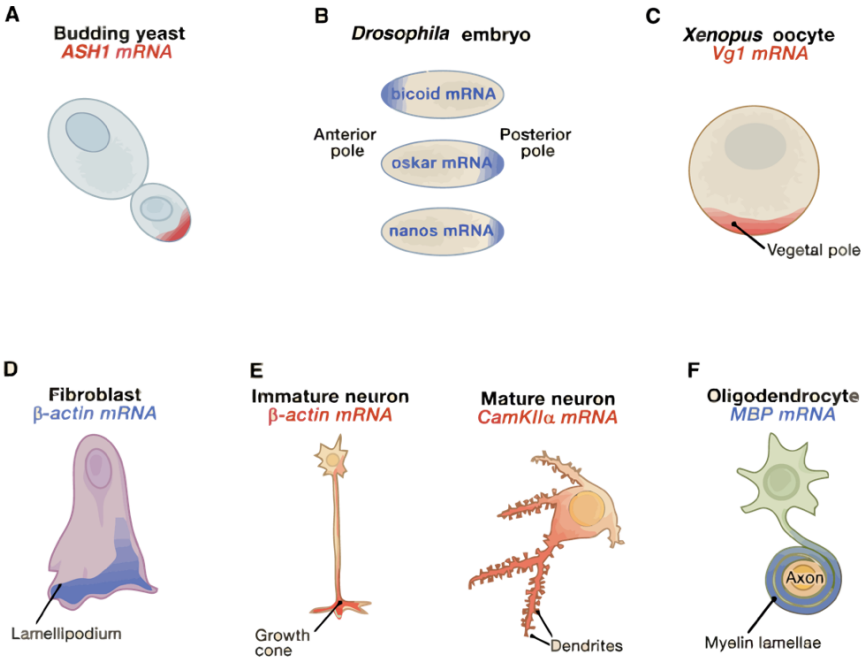

Figure 2. Illustration of to date the best studied examples of mRNA localization and model organisms where localization is studied. (A) Ash1 mRNA localizes to the bud tip of a budding yeast. **(B)** Bicoid mRNA localizes to the anterior pole and oskar and nanos mRNA localizes to the posterior pole of Drosophila embryo. **(C)** Vg1 mRNA localizes to the vegetal pole in Xenopus oocytes. **(D)** Beta-actin mRNA localizes to lamellipodia in chicken and mammalian fibroblasts. **(E)** Myelin basic protein (MBP) mRNA localizes to mammalian oligodendrocyte processes that surround neuronal axons. **(F)** Beta-actin mRNA in present in distal growth cones of developing mammalian axons and CamK2 mRNA is present in distal dendrite of mature pyramidal neurons. Adapted from Cell, 136, 719–730, 2009, Kelsey MC & Ephrussi A. mRNA localization: gene expression in the spatial dimension, Copyright (2009), with permission from Elsevier.

1.2. Neuronal polarity (model system for localization studies)

In eukaryotic cell, targeted transport of various cellular components like organelles, proteins and other molecules including RNAs to distinct sites within a cell, results in cellular polarization (Mellman and Nelson, 2009). Specific cellular domains are formed by Although virtually all of the cells show some polarity and subcellular specialisation (Martin and Ephrussi, 2009), the big distances that separate neuronal processes from the cell body, sometimes several hundred micrometers away, make the isolation of neuronal subcellular domains more feasible and therefore favoured for studies of RNA transport and localized protein synthesis, in general. For a neuronal cell, establishment of polarity is a fundamental property which ensures directional flow of information (reviewed in Arimura and Kaibuchi, 2007.), lead to the formation of structures crucial for reception and transmission of electrical signals, axons and dendrites. Axons - long and thin processes which contain synaptic vesicles with neurotransmitters differ in molecular composition from relatively short dendrites, processes which become thiner more distal from the cell body, ending with the dendritic spines harbouring receptors which receive a neurotransmitter signal. Stimulus-induced changes in the structure and function of these compartments are essential to the formation and plasticity of neural circuits (Kandel, 2001). This changes are brought about by precise local and temporal changes of the proteome in growth cones and synapses, through the mechanisms of neuronal mRNA (transcript) localization and regulated translation up to hundreds of microns from the cell body.

The following chapters will discuss molecular mechanisms together with system level analyses of transcripts localized to neuronal compartments as well as functional relevance of neuronal RNA localization and local protein synthesis.

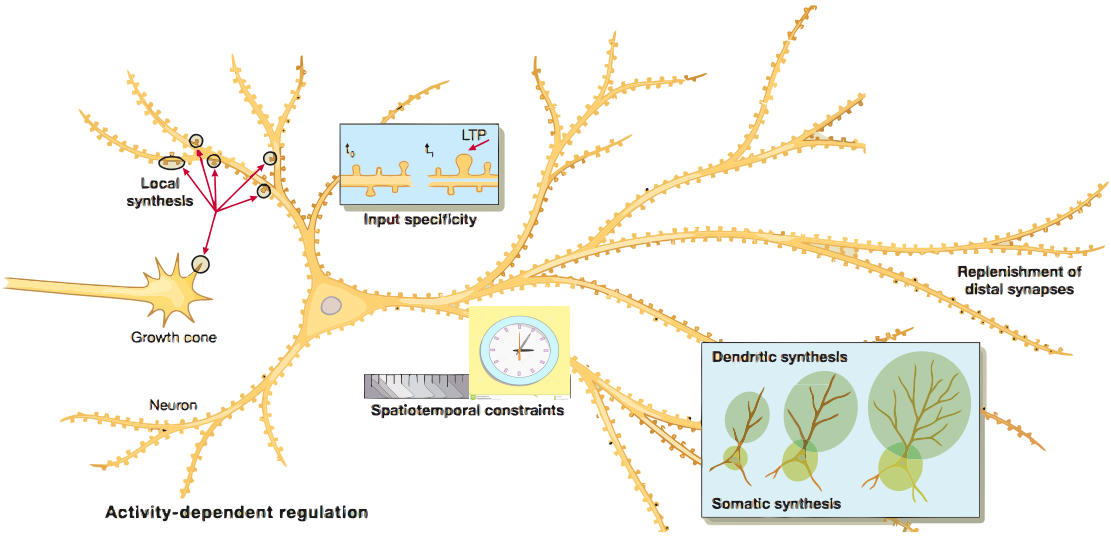

Figure 3. Neuron Size and the Benefits of Local Translation. Size and morphological complexity of neuronal cells poses spatiotemporal limits on cellular metabolism. The capacity of soma may not be sufficient to provide enough proteins for the entire cell. Thus, protein synthesized locally may accumulate over time throughout the entire neuron. Additionally, a role for local synthesis may be to ensure the essential proteins with shorter lifetimes are available within necessary time frame. The impact of local protein synthesis is awaited to be determined by local mRNA levels, translation efficiencies, protein lifespans and local retention. Adapted from Neuron, 81(4): 958-958, 2014. Tom Dieck et al., 2014. Snapshot: Local Protein Translation in Dendrites, Copyright (2014), with permission from Elsevier.

1.3 Newly synthesised protein is required for long-term synaptic plasticity

Brain plasticity refers to the capacity of brain to incorporate changes generated by experience. Internal and external experiences are encoded in the brain as a complex pattern of neural activity leading to the changes in neuronal circuits, brought about by the ability of individual synapses that strengthen or weaken during time in response to neuronal activity that underlies the changes in the synaptic circuitry. Therefore, changes in the strength of synaptic connections, referred as synaptic plasticity are at the core of learning and memory processes and represent a cellular model of learning and memory (reviewed in Citri & Malenka, 2008).

Synaptic activity can be either enhanced or repressed in time window of several milliseconds to hours, days and probably much longer (reviewed in Citri and Malenka, 2008). Short-term changes, last in the order of milliseconds to minutes, resulting in the change in the probability of neurotransmitter release and play a major role in short term behavioural adaptations and short term memory (Citri et Malenka, 2008). However, the new information is stored by long-lasting changes in synaptic activity. The existence of long-lasting changes was first time experimentally confirmed showing repetitive activation of excitatory synapses in hippocampus can potentiate synaptic strength lasting for several days (Bliss and Gardner-Medwin, 1973). The phenomena of long lasting changes in synaptic strength, termed long term potentiation (LTP), together with LTD (long term depression- long lasting changes resulting in the weakening of the synapse), define the concept of bidirectional modification of the strength of synapses by different patterns of activity (Citri & Malenka, 2008), and has been studied as a key to understand molecular and cellular mechanisms involved in memory formation.

Dependence of LTP on protein synthesis was first time demonstrated by Flexner and colleagues (Flexner et al., 1963) when the prolonged injection of protein synthesis inhibitor for several days after learning the task caused the impairment in memory of the mouse. Later, genetic models gave further support for the necessity of new protein synthesis in memory formation, for several different forms of LTP and LTD. (Kelleher et al., 2004, Costa-Mattioli et al., 2005). Soon after, first observation of ribosomes in the distal dendrites of dentate granule cell neurons in electron micrographs (Bodian, 1965, Steward and Levy, 1982) led to speculations that establishment of synaptic contacts and adaptive adjustments of synapses may be driven by local protein synthesis at the synapse.

1.4. Local protein synthesis is required for long-term synaptic plasticity

The initial observation of polyribosomes and several mRNAs species at the distal dendrites, CamKII (Burgin et al., 1990, Mayford et al., 1996), MAP2 (Garner et al., 1988) and b-actin (Tiruchinapalli et al., 2003) suggested that detection of radio-labelled protein in dendrites and biochemical fractions enriched for synapses could be explained by local synthesis (Rao and Steward, 1991; Weiler and Greenough, 1991). In parallel, isolated subcellular compartments like isolated dendrites, axons and synaptoneurosomes were shown to function autonomously, as for growing axons it had been shown they can navigate correctly after soma removal (Harris et al., 1987). The first direct link between synaptic plasticity and local protein synthesis was established by showing that for rapid enhancement of synaptic plasticity, induced by two neurotrophic factors (brain derived neurotrophic factor (BDNF) and neurotrophin-3 (NT-3)), local protein synthesis is required (Kang and Schuman 1996). Later on, numerous studies confirmed that dendrites are a site of protein synthesis

during plasticity, e.g. that the application of BDNF stimulaters protein synthesis of the reporter consisting of a GFP flanked by 5' and 3' untranslated regions (UTR) from CamKII gene, indicating that 3'UTR region contained necessary information for the RNA localization and regulated translation in intact dendrites (Aakalu et al., 2001) or that late-LTP is translation dependent and can be induced and maintained in physical isolation of dendrites from the cell bodies, without influence from somatic protein (Vickers at al., 1998).

In contrast to dendrites, the concept of local protein synthesis in axons, took long time to be accepted, given the evidences that ribosomes in axons, particularly adult axons are limited (Bunge, 1973; Tennyson, 1970). It is known that growing axons *in vivo*, sometimes quite far from soma, make rapid decisions, when they encounter new molecular territories brought about by cues that trigger local rapid changes in protein levels, protein synthesis/ and or degradation (Campbell & Holt, 2001). Transgenic and knockout models gave further support for the roles of local protein synthesis in axonal psychology in directing growth-cone adaptation, gradient signalling, and directional turning in growing axons (reviewed in Perry & Fainzilber, 2013).

1.5 Messenger RNA transport and regulation of local protein synthesis in neurons

Studies over the past two decades have revealed a lot of details regarding the specific ways how the individual mRNAs are localized and ultimately translated within different cell types. Emerged principles support the very first model of ordered pathway of mRNA localisation proposed by Carson and colleagues (Wilhelm and Vale, 1993) where the non-membranous complexes of RNA and RNA-binding proteins (RBPs) are assembled into a functional complex of translationally repressed RNAs in the nucleus, and subsequently translocated to their destinations where they are anchored to the local cytoskeleton by motor-dependent mechanisms. Once at their final destination, the localized RNAs are translated in response to specific stimuli, as it was first time shown for fluorescently labeled myelin basic protein (MBP) mRNA microinjected in cultured oligodendrocytes, which formed granules, that were rapidly transported along microtubules (MT) into processes at a rate of 0.2 mm/s (Ainger et al. 1993) and for the dynamic movements of endogenous RNA granules into dendrites of cultured cortical neurons (Knowles et al. 1996). Transport RNPs displayed rapid anterograde and retrograde trajectories that were dependent on microtubules, consistent with an active RNA transport (Knowles et al., 1996). Further, neuronal RNA granules contain translationally repressed mRNAs that are transported to dendritic synapses, where they are released and translated in response to specific exogenous stimuli (Krichevsky and Kosik, 2001) where after depolarisation, mRNA distribution shifts from heavy granules fraction to the translationally active polysome pool while metabolic labelling of [35S] methionine/mixed amino acids does not correspond to a heavy fraction containing RNA granules, providing evidence that RNA granules are poised in translational arrest, whereas after the induction by diverse stimuli (physiologic, developmental or local), mRNAs redistribute between local mRNPs and translating ribosomes (Krichevsky and Kosik, 2001). Since then, a

plethora of RNAs and RBPs that constitute ribonucleoprotein complexes in neurons have been identified (reviewed in Kiebler and Kosik, 2008).

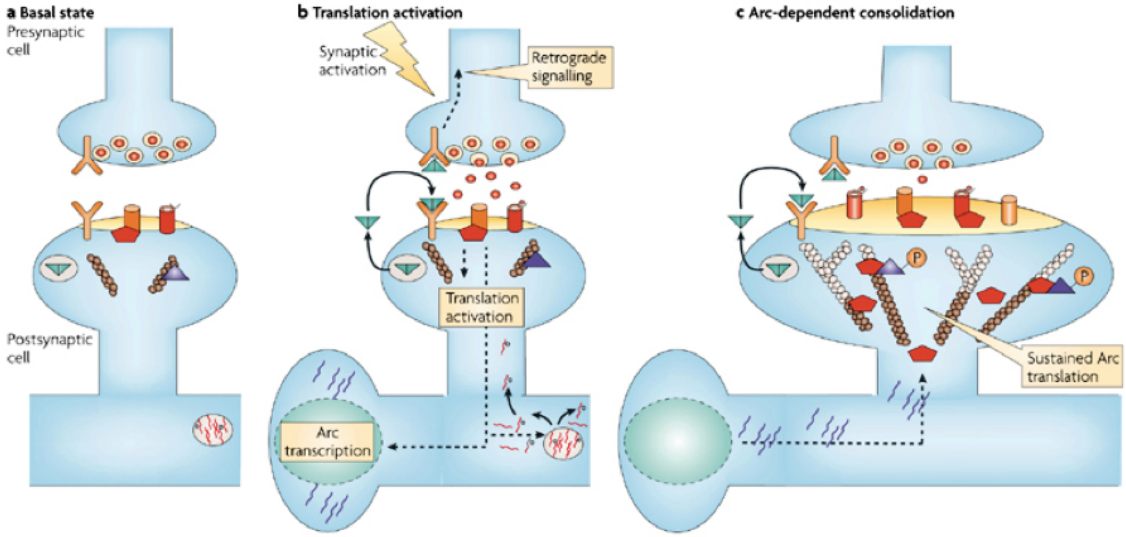

Figure 4. A model of stimulation dependent activation of local translation. (A) neuron in the resting (basal) state, showing mRNA sequestered in an RNA- containing granule. **(B)** High-frequency stimulation (HFS) causes the activation of postsynaptic receptors leading to rapid postsynaptic translation activation. Translation activation is achieved through biochemical regulation of the translation machinery, liberation of mRNA (for example, the mRNA that encodes the α-subunit of calcium/calmodulin-dependent protein kinase II (αCaMKII)) from RNA granules and fine-positioning of the translation machinery, including the translocation of polyribosomes into spines. Spines activated in this way might effectively capture and translate local mRNA pools. **(C)** Arc mRNA is transported to dendrites and locally captured and locally translated. Adapted by permission from Macmillan Publishers Ltd: Nature Reviews Neuroscience **8**, 776-789, 2007. Bramham CR and Wells DG, Dendritic mRNA: transport, translation and function. Copyright (2007).

1.5.3 Neuronal RNA granule composition

How many mRNAs are actually packaged in RNA transport granule and how is granule composition altered by neuronal activity is still not clear. A number of studies suggest that multiple exogenous mRNAs may assemble into a single granule, e.g. mRNAs encoding CaMKIIα, neurogranin (Nrgn), and activity-regulated cytoskeleton-associated protein (Arc) were found to be co-localized in the same set of granules by fluorescence in situ hybridization (FISH) (Tuebing et al, 2010). However, other studies indicate that only a single mRNA is present in a granule (Batish et al., 2012).

However, very recent work from Singer and colleagues (Park et al, 2014) showed that neuronal granules contain multiple β-actin mRNA copies in the soma and proximal dendrites, which are gradually decreasing to a single copy in distant dendrites. Additionally, RNA granules display two events during movement: merge (joining into one granule) and split (separation from a parent granule) while neuronal activity resulted in overall increase in granules as well as in increase of granules containing single β-actin mRNA (Park et al, 2014).

Further, high-resolution imaging of mRNA particles combined with imaging of ribosomes and ribosomal RNA (rRNA) showed that split-merge dynamics of RNA granules occurs during synaptic plasticity to liberate mRNAs for localized expression. The transient increase in mRNA and rRNA in dendrites upon neuron activation, which could be mimicked by treatment with a protease suggested that the increase resulted from unmasking of RNA from RNA binding proteins, or disassembly of granules upon neuron activation. The transient increase in mRNA and rRNA in dendrites upon neuron activation not diminished by application of transcription blockers, showed that unmasked mRNA was transcribed in the soma and then transported to dendrites. Finally, they show the unmasking events correlate with an increase in local β-actin

synthesis (Buxbaum et al,, 2014). In summary, these two studies suggest that the mRNA is in a latent protected state in the granule, which becomes unmasked for translation when the neuron undergoes plasticity (Buxbaum et al,, 2014, Park et al, 2014).

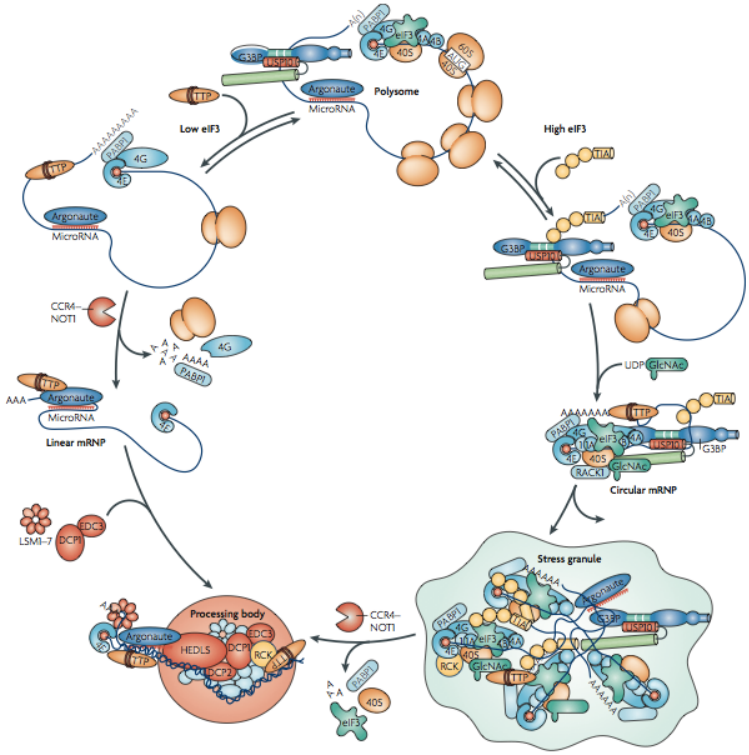

Figure 5. **Dynamic relationship between metazoan Rna granules**. Actively translated polysomal RNA is circularized by interactions between poly(A)-binding protein 1 (PABP1) and eukaryotic translation initiation factor 4G (eIF4G). Polysome disassembly is initiated by deadenylation (left pathway) or by translational silencing (right pathway). Deadenylation results in linearized messenger ribonucleoproteins (mRNPs) which are destined for processing bodies (PBs), subsequently linear mRNA recruits a decapping complex resulting in degradation. Circularized mRNPs are directed to stress granules (SGs) and stay translationally silent. It is also possible that mRNPs in PBs or SGs can be remodelled into other types of RNA granules. Adapted by permission from Macmillan Publishers Ltd: Nature Reviews Molecular Cell Biology, Anderson P and Kedersha N, RNA granules: post-transcriptional and epigenetic modulators of gene expression, Vol 10, 430-436, 2009. Copyright (2009).

1.5.1 Trans-factors

Localization of specific mRNA targets is highly conserved mechanism facilitated mainly by trans factors such as RNA-binding proteins (RBPs) and small regulatory RNAs. The association of RBPs with mRNAs from transcription site until mRNA translation and degradation suggests that RBPs are critical to the spatiotemporal regulation of mRNA expression. RBPs represent a significant fraction of RNA granule (Krichevsky and Kosik, 2001). Characterization of molecular composition of neuronal RNA granules in a more systematic manner using proteomics approaches showed that large RNase-sensitive granule (~1000S in size) are binding partner of conventional kinesin (KIF5) involved in the transport of RNA granules to dendrites and are composed of many mRNA binding proteins that regulate aspects of RNP assembly, translation or stability (Kanai et al., 2003). Based on further studies, granules appear to be heterogeneous, as each protein is not found in all of the granules (reviewed in Thomas et al., 2011). However, very few of these proteins are essential for RNA localization in polarized neurons and only several RBPs have been implicated in the regulation of mRNA transport and translation in neurons, such as cytoplasmic polyadenylation element binding protein 1 (CPEB1), zip code-binding protein (ZBP1), FMRP and Staufen. The identity of these trans-acting factors involved in mRNA trafficking has emerged primarily from in vitro biochemistry approaches, complemented by validation of predicted functions in the brains of specific RBP- knockout mice.

CPEB

The family of cytoplasmic polyadenylation binding protein (CPEB) is RBP which act by binding to the cytoplasmic polyadenylation element (CPE), a cis-element in the 3'-UTRs, to promote cytoplasmic polyadenylation-induced translation in response to synaptic stimulation. The role of CPEB proteins in mRNA transport to dendrites (Richter 2007) was demonstrated in facilitating mRNA transport to dendrites and translational regulation. In rat hippocampal neurons, the CPE incorporated in 3'UTR region of reporter gene is sufficient to direct a reporter RNA into dendrites (Hunag et al., 2003). Although CPEB1 knockout mouse is viable, dendritic transport of a CPE-containing reporter RNA is reduced. (Hunag et al., 2003, Richter 2010). Moreover, CPEB1-null mice have memory deficits and reduced LTP (Alarcon et al. 2004). The complete set of CPEB1 bound transcripts still awaits to be characterized and will be of great interest in further understanding of the actions of this RNABP in neuronal plasticity and, perhaps, neuronal aging.

ZBP

Zip code binding protein (ZBP) whose function was originally demonstrated in studies by Singer and colleagues (Gu et al. 2002) is the most extensively studied RBP involved in dendritic RNA transport and one of the most robust systems developed for understanding the links between mRNA localization in a translationally silent state and its switch to active translation following cell signalling, (Huttelmaier et al. 2005). Further characterization of a consensus binding motif for ZBP1, a bipartite "zip-code" with a defined spacer, has allowed investigators to predict a subset of candidate target transcripts (Patel et al. 2012). It has been observed axonal length and outgrowth was decreased in response to injury in ZBP1 mice, with more systematic studies of ZBP in nervous system ongoing (Donnelly et al. 2011).

FMRP

Fragile X syndrome is the first human neurologic disease attributed to the dysfunction of an RBP. It is caused by triplet repeat expansions in the promoter regions of Fmr1 gene, which results in the loss of expression of FMRP protein (reviewed in Bhakar et al. 2012, O'Donnell & Warren 2002). FMRP, the protein coded by Fmr1 binds to a number of known dendritic RNAs, including MAP1b and PSD95. It is known FMRP exerts multiple functions in mRNA localization and translational repression. Based on the analysis of high-throughput sequencing of cross-linked immunoprecipitated targets (HITS-CLIP), FMRP binds along the coding sequence of a discrete set of mRNAs where it associates with polyribosomes and inhibits translation by causing stalling of ribosome elongation (Darnell et al. 2011) and is transported into dendrites in a neuronal activity-dependent manner. However, mechanism of translational inhibition remains uncertain, with multiple modes of interactions being proposed which may involve different post-translational modifications (Lee et al. 2011, Narayanan et al. 2007) and interaction with miRNAs and other non coding RNAs (Edbauer et al. 2010, Jin et al. 2004, Muddashetty et al. 2011).

1.5.2 Cis- elements

Cis-elements located mainly in the 3' untranslated region (UTR), sometimes also in the 5'UTR or in the coding part of the sequence are the parts of mRNA that regulate its transport to distal parts of neurons. Cis-elements are recognized by diverse trans-acting factors (RBPs and different non-coding RNAs) that often function both in transcript localization and translational regulation. Frequently found as multiple copies of the same element or as a combination of different elements with their length often ranging from a few nucleotides to over 1 kb, with the sequences often forming secondary structures, such as stem loops (Jambrekharr, 2011). Many known localisation elements identified so far regulate mRNA targeting in neurons, among them the best-known examples being the 'zipcode' of b-actin mRNA (Huttelmaier et al, 2005) and cytoplasmic polyadenylation element (CPE), (Huang et al, 2003). In addition, alternative RNA processing, apart from generating diversity in the cellular proteome; can also generate alternative UTRs, resulting in the transcripts containing either a shorter 3'UTR lacking or longer 3'UTR containing regulatory regions that can affect mRNA translation, stability as well as RNA localisation (Di Giammartino et al., 2011). Brain derived neurotrophic factor (BDNF) is the best studied example of how alternative polyadenylation generates mRNA isoforms with different subcellular localization patterns (Will et al., 2013). While distinct promoters of BDNF gene are responsible for tissue-specific expression, additionally transcripts can be polyadenylated at two alternative sites, producing mRNAs with 3'UTR of different lengths, with longer UTR directing dendritic localization of the longer isoforms (Timussk et al., 1993). Similar to BDNF, a longer isoform of myo-inositol monophospatase (Impa1) with additional element in 3'UTR is localized and translated in distal axons, more than 1600 mm away from the cell bodies, whereas an isoform with a shorter 3'UTR remains mostly localized to the cell bodies (Andreassi et al 2010).

1.6 Dendritic transcriptome

Characterization of all the RNAs present in the distal region. is essential to fully understand the mechanisms and functional relevance of dendritic RNA localization and local translation. Rapid development of high-throughput RNA profiling techniques has enabled genome-wide transcriptome analyses to be performed on isolated axons and dendrites in a variety of neurons. To date, major technical difficulty in such analysis lies in obtaining pure and sufficient quantities of dendrites and axons for analysis while excluding the possibility that the signal is a result of a cell-body contamination. For i*n vivo* profiling studies, neuropil segments of the adult rodent hippocampus are used since they consists of dendrites, axons, glia, and a sparse population of interneurons, but lack the neuronal cell bodies. For the *in vitro* analyses of primary neuronal cells, more recently developed methodologies include the use of compartmentalised chambers in which the processes (dendrites or axons) are (mechanically or fluidicaly) isolated from cell bodies (Taylor et al., 2010) together with laser capture microdissection. approaches. (Zivraj et al., 2010).

Current estimate, from two genome-wide independentl studies is that more than half of the neuronal cell's transcriptome can be detected in axons and dendrites. (Kamme et al., 2003 and Cajigas et al., 2012). The first study, based on microarray, estimated the number of localized transcripts to be around 4,500 (Kamme et al., 2003) while recent work using 454 sequencing showed similar result, i.e. around 2,550 genes were detected in hippocampal neuropil (Cajigas et al., 2012). These numbers suggest that a substantial fraction of the total cellular proteome functions in the dendritic and axonal subcellular compartments. Schuman and colleagues (Cajigas et al., 2012) argue that this concept is feasible since the volume of axons and dendrites is about 30–60 times greater than that of the soma. The study of the individual gene *Camk2a* further

supports the claim that a substantial fraction of the dendritic and synaptic proteins may be translated locally. When *Camk2a* mRNA was deleted from dendrites, that resulted in an 85% loss of the synaptic CaMKIIa protein (Miller et al., 2002).

The fraction of neuronal non-coding transcriptome that is localized within dendrites and axons is largely unknown since the recognition of functional RNA classes that do not encode proteins came relatively recently. To date, the systematical approaches to address the presence of those classes of RNA in neuronal processes are very few (Picardo-Chrass, 2012, Siegel et al., 2009), but general agreement is that, these noncoding RNAs also exist and are potentially enriched in neuronal compartments (Holt, Schuman, 2013).

1.6.1 Dendritic mRNAs

The prerequisite for local protein synthesis to occur is that mRNAs and translation machinery components are present locally. The quest for specific mRNAs that could be translated locally, in dendrites and axons started after the discovery that local protein synthesis is essential in carrying out mechanisms of synaptic plasticity (Kang, Schuman 1996). First individual mRNAs detected in dendrites were visualized by *in situ* hybridization techniques, including the mRNA for the Ca-calmodulin- dependent protein kinase alpha subunit, CaMKIIa (Burgin et al., 1990; Mayford et al., 1996), MAP2 (Garner et al., 1988), Shank (Böckers et al., 2004), and b-actin (Tiruchinapalli et al., 2003). Afterwards, the systematic microarray profiling further advanced the detection of localized transcripts (Poon et al., 2006; Zhong et al., 2006) but only with the introduction of novel RNA sequencing technologies, the local transcriptome in dendrites and axons has been dramatically expanded. The number of transcripts identified in CA1 neuropil reached 2,550 (Cajigas et al., 2012), based on the extensive

in situ hybridization validations of the transcripts detected by deep sequencing. Beside the unexpectedly big number of mRNAs detected in CA1 neuropil, the work from Schuman and colleagues also showed there is a big difference in the abundance (over three orders of magnitude) and distribution of detected mRNAs. Three main groups of mRNA were defined based on the difference in the distribution along the proximal to distal dendrite axis (Cajigas et al., 2012).

The current repertoire of neuropil mRNAs includes mRNAs for most protein families represented in Gene ontology (GO). Expectedly, mRNAs for different classes of synaptically relevant proteins including ionotropic and metabotropic neurotransmitter receptors, adhesion molecules, synaptic scaffolding molecules and signaling molecules are present, as well as the components and regulators of the protein synthesis and the degradation machinery (Cajigas et al, 2012). Local mRNA regulation has also been linked to neurological and neurodevelopmental disorders characterized by intellectual disabilities, brain hyperexcitability, and neurodegeneration (Wang et al., 2007). The localization of many mRNAs relevant for these diseases including Fmr1 and Fxr1 and Fxr2 relevant to Fragile X syndrome, Nlgn1,3, and Shank3 in Autism-spectrum disorders and Snca for Alzheimer's disease within the processes suggests that disregulation of mRNA localization or translation may give rise to some of the phenotypes associated with these diseases (Cajigas et al., 2012).

1.6.2 Dendritic non-coding RNAs

The introduction of deep sequencing in RNA profiling enabled the detection and appreciation of many different non-coding RNA (ncRNA) species. Non-coding RNAs represent a heterogenous group of RNA transcripts containing dozens of distinct

classes of ncRNA transcripts, which do not code for proteins but are proved to or believed to be funcitonal. According to the laboratory techniques used for size fractionation of isolated RNA, ncRNAs are loosely grouped into small ncRNAs (<200 nt) or long ncRNAs (>200 nt). The classification is further challenged by transcripts with both coding and non-coding functions (reviewed in Ulitsky and Bartel, 2013). The functions of several individual ncRNAs elucidated to date, suggest they might play important roles in gene regulation and other cellular processes (Mercer et al., 2013) though very little is known about their function in neurons (Qureshi and Mehler, 2012). However, the fact that the majority of transcribed eukaryotic genome is non-coding and that more than the half of the neuronal mRNA population is localized to axons and dendrites (Cajigas et al., 2012), indicates possible existence and enrichment of ncRNAs in neuronal compartments.

To date, the most widely studied group of neuronal ncRNAs are microRNAs (miRNAs), small ncRNAs involved in post-transcriptional regulation of target RNAs via mechanisms of RNA interference (Fiore et al., 2011). MicroRNAs bind to imperfectly complementary sequences, predominantly in 3′-UTRs of target mRNAs, leading to repression or degradation of the transcripts. (Selbach et al., 2008, Guo et al., 2010). On one hand, individual miRNA can regulate hundreds of different mRNAs, on the other hand, multiple miRNAs target a single mRNA (Ameres and Zamore, 2013). Only a handful of miRNAs are known to regulate different synaptic functions (reviewed in Schratt, 2009). From several genome-wide studies addressing the miRNA distribution in different brain regions and within subcellular compartments showed that distribution of miRNAs through the somatodendritic compartment is in a nearly constant gradient with only a very small number of miRNAs deviating as relatively enriched or depleted in the dendrite (Kye et al., 2007, Pichardo-Casas et al., 2012). For several miRNAs the copy number in individual neurons and in dendrites was estimated to be as high as 10,000—equivalent to the

number of synapses of a typical pyramidal neurone (Kye et al., 2007). However, the model for understanding miRNA processing and mechanism of action is still developing. Several important questions remain yet to be answered, one being the regulation of the miRNAs themselves. It has been shown that other, additional RNA classes can regulate miRNA function (Memczak et al, 2013, Salmena et al., 2011) as in the case of a circular RNAs antisense to a cerebellar degeneration protein (CDR1/ cir-7), (Memczak et al.2013, Hansen et al.2013) shoen to function as a sponge for miR-7, adding circular RNAs to the pool of non-coding RNAs with potential for diverse regulatory functions in neurons. Further, among the very few known examples is rodent brain cytoplasmic RNA Bc1, a non-coding RNA that is actively transported to the somato-dendritic domain of neurons where it functions as a repressor of local protein synthesis by disrupting the assembly of translational initiation complex (Zhao et al., 2013).

Complementary classification ncRNAs is according to their genomic location, where ncRNAs are transcribed in antisense, overlapping, intronic and bidirectional orientations relative to protein coding genes; from gene regulatory regions (UTRs, promoters and enhancers); and from specific chromosomal regions (telomeres) (Ulitsky and Bartel, 2013).

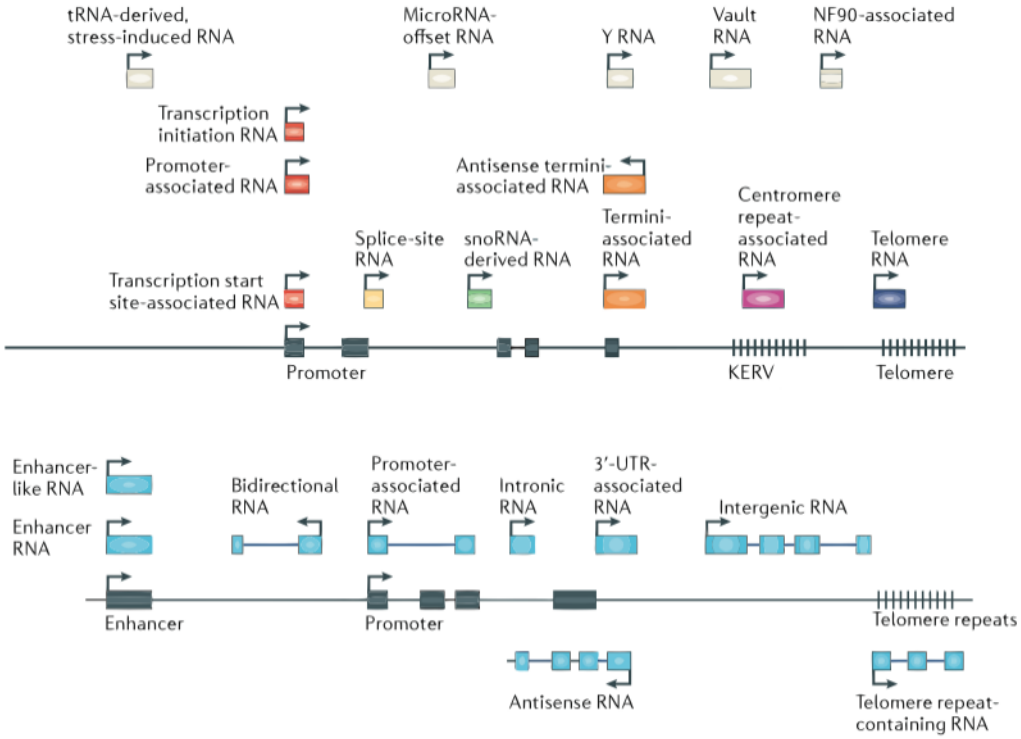

Figure 6. Emerging classes of non-coding RNAs. (A) Long non-coding RNAs (lncRNAs; shown in blue) mediate a wide range of genomic and cellular functions. They are independently transcribed from regulatory regions in the genome including promoters, enhancers and untranslated regions (UTRs); as well as from specific chromosomal regions including telomeres. Transcriptional orientation can be bidirectional, antisense, intronic and overlapping to protein-coding genes (black), arrows indicate direction of transcription. **(B)** Small ncRNAs are derived from protein-coding gene (black) regulatory regions, including 5′ regulatory regions (red), gene ends (orange), intron– exon junctions (yellow) and introns (green). They are also derived from specific chromosomal regions, centromeres (purple) and telomeres (blue), and can be splicing products of other ncRNAs. Adapted by permission from Macmillan Publishers Ltd: [Nature Reviews Neuroscience] (Emerging roles of non-coding RNAs in brain evolution, development, plasticity and disease, Qureshi IA and Mehler MF, 2012; 13(8): 528-41). Copyright (2012).

1.7 Circular RNAs

Circular RNAs (circRNA) are a heterogenous group of RNAs formed as a result of a "head to tail " splicing, by covalent binding of a 3' end of a downstream exon and 5' end of an upstream exon of a same RNA molecule. CircRNAs have been known to exist since the first electron microscopy observation, two decades ago (Hsu MT and Coca-Prados M, 1979). With only a handful of genes found to express circular transcripts and without clear function attributed to any of them, until very recently circular RNA transcripts were considered to result from erroneous splicing and to be of low abundance (Zaphiropoulos et al.,1996). Deep sequencing of ribosome-depleted RNA, combined with computational tools has led to the identification of thousands of new cRNAs in organisms ranging from Archea to human (Salzman et al., 2012) with large numbers of them stably abundant in mammalian cells (Memtzak et al., 2013), transcribed from diverse genomic locations (for example, from coding and non-coding exons, intergenic regions or transcripts antisense to 5' and 3' UTRs) in a complex tissue-, cell-type- or developmental-stage- specific manner, with the majority of them being transcribed from genomic locations known to encode a linear mRNA (Memczak et al.2013).

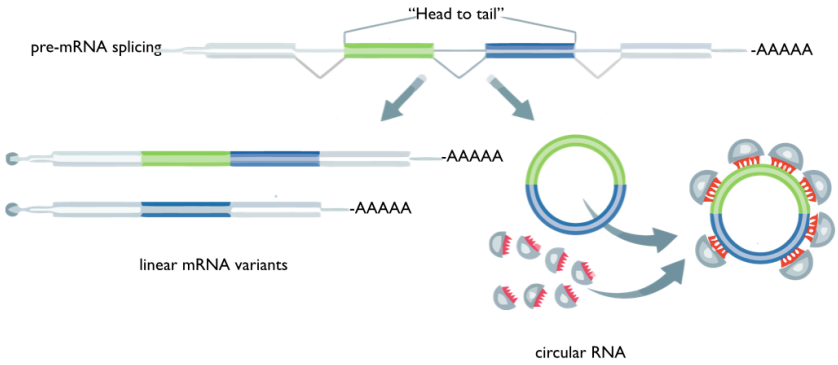

Figure 7. Schematic representation of circular RNAs biogenesis. A gene can be transcribed and spliced into linear and circular isoform. Colour boxes and solid lines represent exons and introns respectively. **(A)** Linear transcripts consist of constitutive and alternatively spliced exons in a consecutive order. Green and blue boxes indicate constitutive and alternative exon respectively. **(B)** Circular RNAs contain the unique 'head to tail' splice junctions formed by an acceptor splice site at the 5' end of an exon and a donor site at the 3'end of a downstream exon. First described role for circRNA is to act as a microRNA sponge by densely binding Ago-miRNA complex. Adapted by permission from WILEY: EMBO Journal. Circular RNAs: splicing's enigma variations, Hentze MW & Preiss T, 2013; 32(7): 923-5. Copyright © 2013 European Molecular Biology Organization.

1.7.1 Circular RNA detection

Observation of backsplice sequences is crucial evidence of exonic cRNA production. However, cDNA sequences consistent with back splicing can be produced by experimental artifacts and other molecular mechanisms, as reverse transcriptase template switching, tandem duplication or RNA trans-splicing (Cocquet et al., 2006). Nevertheless, such events are considered to be rare and not expected to contribute to the abundant cDNA molecules with such aberrant pattern. In genome-wide approach, cRNAs can be identified by deep sequencing of ribosome depeleted total RNA. The presence of cRNA can be indicated by identification of independent mapping of paired-end reads, where two read pairs mapped to the same gene but in the opposite

order from that expected based on genome reference sequences. Additionally, the existence of cRNA identified by this approach could be supported experimentally by showing the resistance of circRNAs to RNaseR exonuclease treatment using Northern blot and qPCR with divergent primers, using primers that are oriented to amplify away from each other in the genmoic sequence resulting in no product but only in the case of backsplicing become convergent and amplify a discrete amplicon (reviewed in Jeck et al., 2014).

1.7.2 Circular RNA features

CircRNAs are a heterogeneous group of transcripts, very stable in cells with an average half-life of more than 48h (Jeck et al., 2013), compared to average mRNAs half-life of 10 h (Schwanhäusser, B. et al., 2011). This may result in even higher levels of some circRNA transcript in the cell than of the linear transcript from the same loci (Salzman et al., 2013, Jeck et al., 2013). Localization studies using different approaches show circRNAs have predominantly cytoplasmic localization (Jeck et al., 2013, Hansen et al., 2011). Although previously thought to be of a very low abundance, the estimates of absolute abundance of circRNAs in the total pool of RNA has been recently revisited, suggesting that the substantial fraction of non ribosomal RNA is circRNA (Jeck et al., 2013, Salzman et al., 2013). Two mechanisms have been proposed for mammalian exonic cRNA formation, both of them involving canonical spliceosome complex for back splice formation. First mechanism is that downstream splice donor pairs with an non-spliced upstream splice acceptor (Cocquerelle et al., 1996) and the RNA is circularized. The second mechanism is known as “exon” skipping mechanism and involves splicing within byproducts produced from exon

skipping (Gualandi et al., 2003). So far, more evidence was found in support of the backsplice theory, although some linear RNA has been found that lack exons included in circular RNA (Zaphiropoulos et al, 1997) leaving it a plausible model, although for the majority of cRNAs, genome wide studies have failed to find such linear RNAs. Interestingly, circRNA production is regulated independently of the underlying linear RNA gene and together with the abundance and evolutionary conservation suggest exonic cRNAs might have specific roles in cellular physiology with a number of possible functions being proposed by now.

1.7.3 Potential functions of circular RNAs

A spectrum of proposed mechanisms includes involvement in transcription, as well as sequestration, storage, sorting or localisation of RBPs (Hentze and Preiss, 2013). For example, a function proposed for circularisation of formin gene (Fmn), a gene essential in limb development is sequestration of the translation start site, and thereby reduction the protein expression (Chao et al., 1998). This would suggest potential functions for circRNAs through their mechanism of formation, rather than as end products. It is possible also that circular RNAs could sequester RBPs and thereby could also regulate the intracellular transport of associated miRNAs, RBPs, or mRNAs (Hentze and Preiss, 2013). For example, cRNA can stably associate with AGO proteins and RNA polymerase II (Jeck et al.,2012, Memczak et al., 2013) or instead of acting as a repository for microRNAs, circRNAs could be involved in their intracellular transport including the possibility for the timed release of the circRNA cargo as shown for the ability miR-671, to trigger slicing of CiRS-7 (Hansen et al, 2011). CircRNAs could also function more broadly to store, sort or localize RBPs. Some further models would be assembly or regulation of ‘RBP factories’, such as the

recently recognized enzymes of metabolic pathways with RBP activity (Castello et al, 2012), or could potentially serve as their allosteric regulators. Finally, the ability of circRNAs to function as templates for protein synthesis is also possible since inclusion of an internal ribosomal entry site (IRES) allows translation of engineered circRNAs. (Chen and Sarnow, 1995). However, the coding potential of many ATG containing circular RNAs has been considered, but to date all efforts (Jeck et al. 2012, Salzman et al., 2013) did not result in identification of exonic circRNA bound to polysomes, neither in peptides identified in mass spectrometry data that would correspond to a translational product of exonic circRNAs. To date, the only functionally characterized circRNAs function as miRNA sponges or competing endogenous RNAs, i.e. decoys for the binding of miRNA with their coding targets. The capacity for sponging was already previously reported (reviewed in Ebert and Sharp 2010) for exogenous linear transcripts that harbour microRNA target sites that could 'sponge up' or inhibit an endogenous microRNA when artificially expressed in the cells. Both Rajewsky and Kjems lab found CDR1as/ciRS-7 as a highly expressed endogenous circular RNA with more than 70 conserved miR-7 target sites, functioning as microRNA sponge (Memtzak et al., 2013,Hansen et al., 2013). Further, they showed that CDR1/ciRS-7 is densely bound by Argonaute protein using PAR-CLIP and HITS CLIP. Additionally, transcript copy number estimation suggests that CDR1as/ciRS-7 could sponge a significant fraction of the miR-7 population. Another example of microRNA sponge is the circular isoform of a well studied mouse SRY gene (Hansen et al., 2013), a single exon, sex-determining gene in males. During development, the SRY RNA exists as a linear transcript that is translated into protein, while in the adult testes, the RNA exists primarily as a circular product that is predominantly localized to the cytoplasm and is apparently not translated (Dubin et al., 1995). There are 16 putative target sites for miR-138 and analogous experiments

to CDR1as/ciRS-7 to showed that circular isoform of SRY gene can functions as a sponge for mir-138 (Hansen et al., 2013).

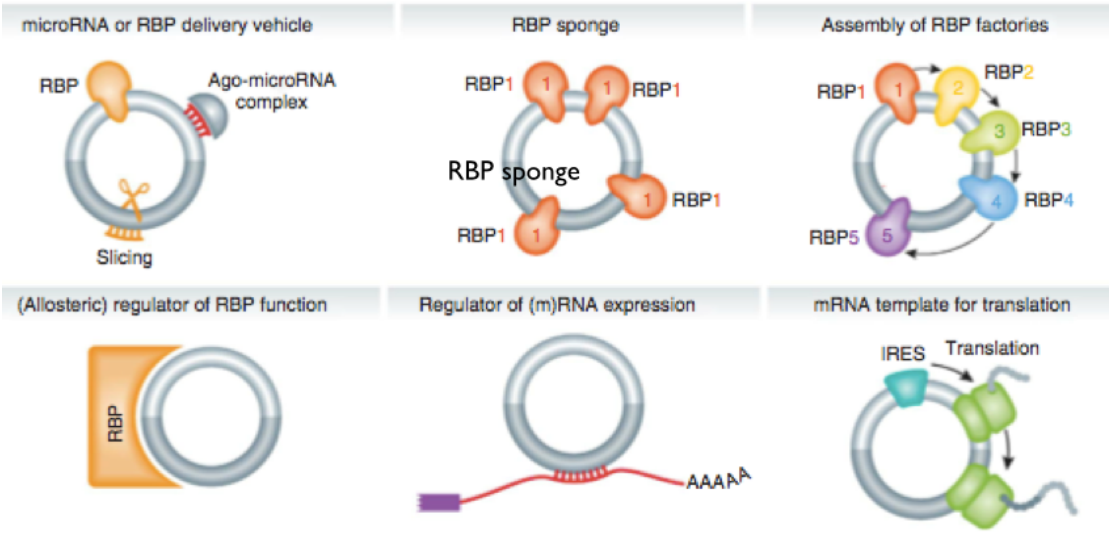

Figure 8. Potential roles of circular RNAs. (**A)** Circular RNAs could be involved in miRNA transport., with a possible mechanism for the timed release of the circRNA load. **(B)** Circular RNAs could function more broad to store and localize RBPs. **(C)** CircRNAs as regulators of RBP assemblies with certain function like enzymes of metabolic pathways with RBP activity (Castello et al., 2012). **(D)** CircRNAs as allosteric regulators. **(E)** Circular RNAs could function to direct mRNAs to specific location by partial base pairing **(F)** It is also possible circRNA could function as templates for protein synthesis since IRES (internal ribosomal entry site) are present on some RNAs. Adapted by permission from WILEY: EMBO Journal. Circular RNAs: splicing's enigma variations, Hentze MW & Preiss T, 2013; 32(7): 923-5. Copyright © 2013 European Molecular Biology Organization.

1.8 Aims of this PhD Thesis

Overall aims of this PhD thesis are;

- To establish synaptosome purification protocol for downstream RNA profiling using high-throughput sequencing approaches

- To determine the gene expression profile of protein-coding genes in synaptic fraction from mouse hippocampal synaptosomes compared to the whole hippocampus

- To determine non-coding circular RNA gene expression profiles

    1. across different mouse tissues

    2. across different developmental stages of mouse brain

    3. in neuronal compartments (subcellular localization)

    4. in response to neuronal stimulus

- To biochemichally characterize one circularRNA candidate

2. MATERIALS

2.1 Chemicals and consumable

Chemical / consumable	Supplier
1.4 Dithiothreitol	Carl Roth, Germany
2- Mercaptoethanol	Sigma-Aldrich, Germany
20% SDS	Carl Roth
2-Propanol HPLC-Grade	Carl Roth, Germany
4 – 12% NuPAGE gradient gel	Invitrogen, USA
40% Acrylamide 19:1	Bio Rad, USA
Acetic Anhydride	Sigma-Aldrich, Germany
Acid Phenol Chloroform	Ambion, USA
Agarose	Invitrogen, USA
Agencourt AMPure XP beads	Beckman Coulter, USA
Agencourt RNAclean XP beads	Beckman Coulter, USA
Bench Mark Protein Ladder	Invitrogen, USA
BSA	Roche Diagnostics,
Calciumchloride	Merck, Germany
Centrifuge tubes 15mL and 50mL	Falcon, USA
Chloroform 99%	Sigma-Aldrich, Germany
C18 beads	Invitrogen
DAPI	Sigma-Aldrich, Germany
Difco Agar	BD, USA
DIG RNA labeling mix	Roche Diagnostics,
DNA Ladder 100bp	New England Biolabs
DNA Polymerase I	Invitrogen, USA
dNTPs 100mM	Invitrogen, USA
EDTA	Carl Roth, Germany
Ethanol absolut	Merck, Germany
Ethidium bromide	Merck, Germany
Formaldehyde 37%	Carl Roth, Germany
Formamide, deionized	Sigma-Aldrich, Germany
Glycerol	VWR, Germany
GlycoBlue	Ambion, USA
Glycogen	Ambion, USA
HCl 1N	Carl Roth, Germany
Hepes- sodium salt	Sigma-Aldrich, Germany
Hybond TM N+ Membrane	Amersham, USA
Hybond TM P Membrane (PVDF)	Amersham, USA

Hydroxyperoxide	Sigma-Aldrich, Germany
Isopropanol	Sigma-Aldrich, Germany
KOH 5N	Sigma-Aldrich, Germany
Magnesium chloride	Fisher Scientific, USA
Methanol HPLC-Grade	Sigma-Aldrich, Germany
Microscope slides poly-Lysine treated	Sigma-Aldrich, Germany
NaOH 10M	Invitrogen, USA
Nonidet P 40 Substitute	Invitrogen GmbH
NuPAGE LDS loading buffer	Carl Roth, Germany
PBS	Carl Roth, Germany
Percoll	GE Healthcare, USA
Percoll PLUS	GE Healthcare, USA
Ponceau S	Sigma-Aldrich, Germany
Potassium acetate	Sigma-Aldrich, Germany
Potassium chloride	Carl Roth, Germany
Potassium Phosphate	Roche, Germany
Propidium iodide	Epicentre Biotechnologies,
Proteinase K	Carl Roth, Germany
RNAse R	Invitrogen, USA
RNase AWAY	Ambion, USA
RNaseH	Carl Roth, Germany
Siliconized Tubes 1.5mL and 2mL RNAse	Carl Roth, Germany
Sodium Acetate anhydrous	Sigma-Aldrich, Germany
Sodium chloride	Sigma-Aldrich, Germany
Sodium Hydroxide	Sigma-Aldrich, Germany
SSC Buffer 20x concentrate	Applied Biosystems, USA
Streptomycin sulfate	New England Biolabs GmbH
SYBR-Green qPCR Mastermix	Roche Diagnostics, GmbH
T4 DNA Ligase	Carl Roth, Germany
T7 Polymerase	Carl Roth, Germany
Tris (base) 99,9%	Carl Roth, Germany
Tris HCl 99,9%	Invitrogen GmbH
Triton X100	Invitrogen GmbH
Trizol LS Reagent	Invitrogen GmbH
Trizol Reagent	Carl Roth, Germany
Trypsin EDTA	Carl Roth, Germany

2.2 Equipment

Kit	Manufacturer
36 Cycle Illumina Sequencing Kit cDNA	Illumina, USA
Superscript III DNA 1000 Chip Kit	Invitrogen, USA
Dynalbeads mRNA Purification Kit	Invitrogen, USA
Illumina Sequencing Kit	Illumina, USA
Illumina Standard Cluster generation kit	Illumina, USA
Paired-End Cluster Generation Kit	Illumina, USA
Paired-End DNA Sample Prep Kit	Illumina, USA
RNA 6000 Pico Chip Kit	Agilent, USA
RNA 6000 Nano Chip Kit	Agilent, USA
DNA 1000 Chip Kit	Agilent, USA
Second strand synthesis kit	Invitrogen, USA
SYBR-Green RT-PCR kit	Applied Biosystems

Equipment	Manufacturer
Agarose gel electrophoresis chambers	PeqLab, Germany
Agilent 1200 LC System	Agilent Technologies, USA
Axio Observer Z1 Fluorescence microscope	Zeiss, Germany
Bioanalyzer 2100	Agilent Technologies, USA
Centrifuges	Eppendorf, Germany
Cluster station	Illumina, USA
Leica SP2 Confocal Laser Scanning Microscope	Leica Lasertechnik,
Genome Analyzer High Seq Sequencer	Illumina, USA
Heat and stirring plate	VWR, Germany
Illumina Cluster Station	Illumina, USA
Incubators	Sanyo, Japan
LTQ-Orbitrap (Classic, XL and Velos) MS	Thermo Fisher, USA
Microcentrifuge	VWR, Germany
NanoDrop ND-1000	Nanodrop Technologies,
PCR thermal cycler	Bio Rad, USA
Pipetboy comfort	VWR, Germany
Pipettes (10µL, 100µL, 200µL, 1000µL)	Gilson, USA
Power supplies	Bio Rad, USA
Protein electrophoresis chambers	PeqLab, Germany
Shaking incubators	New Brunswick, USA
StepOnePlus qPCR cycler	Applied Biosystems, USA
Thermomixer compact heatblock	Eppendorf, Germany
UV transluminator	UVP, USA
Vacuum concentrator	Eppendorf, Germany
Vortex Genie 2	VWR, Germany

3. METHODS

3.1 Experimental Methods

3.1.0 Tissue collection and hippocampal dissections

For the developmental studies, hippocampi were dissected from wild type C57B6 mice at the age of E18, P1, P10 and P30. For tissue profiling wild type C57B6 mice at the age of 14 weeks were used to dissect the brain, liver, lung, heart and testes. All tissues were subsequently lysed in Trizol (Invitrogen) to extract RNA following the manufacturer‟s instructions.

3.1.1 Purification of synaptosomes

Synaptosomes were purified from mouse young adults (four to six weeks old) as previously described (Dunkley et al., 2008). Four to six weeks old mice (C57BL/6) were decapitated, and their brains were rapidly removed. The cortex and hippocampus were homogenized in ice-cold sucrose buffer (320 mM Sucrose, 5 mM HEPES, pH 7.4) with a glass- Teflon homogenizer. Homogenate was subjected to two differential centrifugations (1,000 g for 10 min and 12,000 g for 10 min). Pre-made, refrigerated, discontinuos Percoll sucrose gradients (3%, 10%, 15% and 23% Percoll Plus in sucrose buffer at 31,000 g) were loaded with 2 ml of 5 mg/ml homogenate before applying a centrifugation with a Sorvall type SS-34 refrigerated angle-head rotor for 5 min. The latter resulted in separation into five different fractions. The fraction at the interface of the 23% and 15% Percoll Plus contained the most pure fraction of synaptosomes and was therefore used for all experiments performed in this study. Synaptosomes were pelleted at 30,000 g in HBSS buffer and used for downstream experiments or total RNA was isolated by Trizol.

3.1.2 Total RNA extraction

Total RNA from all tissues used in the study was extracted by TRIzol following the manufacturer's protocol. Briefly, 1 ml of TRIzol reagent (Invitrogen) was added per 50- 100 mg of tissue lysate. The tissue lysate in TRIzol was homogenized by passing through a 26 G needle 8-10 times and incubated at room temperature for 5 min. After homogenization, 0.2 ml of chloroform was added to per mL TRIZOL lysate and mixed by vigorous shaking for 15 sec. The mixture was incubated at room temperature for 3 min, transferred to a pre-spun 2ml Phase-Lock-Gel tube (5 Prime), and centrifuged at 18,000 x *g* for 15 min at 4°C to separate phase. The upper aqueous phase containing RNA was carefully aspirated to a fresh, nuclease-free tube. The RNA was then precipitated by adding one volume of isopropanol and 1/10 volume of 5 M NaCl, and centrifuged at 18,000 x *g* for 10 min at 4°C. Finally, the RNA pellet was washed with 75% ethanol, air-dried and dissolved in nuclease-free water. The dissolved total RNA was quantified by NanoDrop (NanoDrop Technologies) and the quality was assessed by Agilent 2100 Bioanalyzer (Agilent Technologies) according to the manufacturer's instructions.

3.1.3 PolyA and rRNA depleted RNA sequencing library preparation

PolyA RNA sequencing was performed using 500 ng total RNA following Illumina mRNA- Seq library preparation protocol (Illumina) as illustrated in Figure 2.2a. Briefly, poly(A) RNA was isolated by two rounds of oligo (dT) Dynabeads (Invitrogen) purification. Purified poly(A) RNA was fragmented at 94 C for 3.5 minutes using 5 x fragmentation buffer (200 mM Tris-Acetate, pH 8.1, 500 mM KOAc, 150 mM MgOA), as described in (Adamidi et al. 2011). The fragmented RNA were purified by Agencourt RNAClean XP SPRI beads (Agencourt, A63987) and converted to first strand cDNA using random hexmer primer (Invitrogen) and Supescript II (Invitrogen), followed by second strand cDNA synthesis with E.coli DNA pol I (Invitrogen) and RNAse H (Invitrogen) and Agencourt AMPure XP beads

(Agencourt) purification. Stranded rRNA depleted sequencing was performed using 500 ng total RNA following Illumina Tru-Seq Stranded library preparation protocol (Illumina). Briefly, total RNA was mixed with RNA Binding Buffer and rRNA removal Mix and denatured 5 min at 68C. The rRNA was removed with rRNA removal beads. The non ribosomal RNA form supernatant was further purified by Agencourt RNAClean XP SPRI beads (Agencourt, A63987). Fragmentation and random hexamer priming was done simultaneously at 94°C for 8 minutes and converted to first strand cDNA using random hexmer primer (Invitrogen) and Supescript II (Invitrogen), followed by second strand cDNA synthesis with E.coli DNA pol I (Invitrogen) and RNAse H (Invitrogen) followed by Agencourt AMPure XP beads (Agencourt) purification.

Sequencing libraries were prepared from purified double stranded (ds) cDNA either automatically using SPRI-TE Nucleic Acid Extractor (BECKMAN COULTER) following the manufacturer's instructions, or manually using NEBNext DNA Library Prep. Kit (NEB). In short, the double stranded cDNA was end repaired, A-tailed and ligated with Illumina paired end sequencing adaptors (Illumina). Each step was purified by Agencourt AMPure XP SPRI beads (Agencourt). The purified ligated product were amplified by Phusion polymerase with the following PCR program: 98°C 30 sec, (98°C, 10 sec, 65°C 30 sec, 72°C 30 sec) x 15 cycles, 72°C 5 min, 4°C hold. The PCR product was then purified by Agencourt AMPure XP beads (Agencourt) as the sequencing library. The prepared library was quantified by Qubit using DNA HS kit (Invotrogen), quality assessed by Bioanalyzer (Agilent) and sequenced on Illumina HiSeq in single-end and paired-end mode depending on the sample, following the standard protocol.

3.1.4 Electron microscopy

For electron microscopy, synaptosomes were collected onto Isopore filters and immediately fixed in 4% (w/v) PFA and 1% (v/v) glutaraldehyde in 0.1 M phosphate buffer (pH 7.4) for 30 min on ice. The filters were then washed, osmicated for 1 h (1% OsO4), dehydrated through a graded series of ethanol, including a step of 1.5 h in 70% ethanol with 1.5% uranyl acetate, and embedded in Epon. Ultrathin sections (60 nm) were stained with uranyl acetate and lead citrate and examined with a Zeiss EM 902. Digital images were taken using a ProScan CCD camera. Following export, images were processed manually using ImageJ software.

3.1.5 High-Resolution RNA In Situ Hybridization and Immunostaining

High resolution *in situ hybridization* was performed as previously described (Cajigas et al). In brief, hippocampal neurons were prepared and maintained as described in (Aakalu et al., 2001). In situ hybridization was performed using the QuantiGene (QG) ViewRNA kit from Panomics as previously described (Taylor et al., 2010) with the following modifications. Cells (DIV 18-24) were fixed for 30 min at room temperature using a 4% paraformaldehyde solution (4% paraformaldehyde, 5.4% Glucose, 0.01 M sodium metaperiodate, in lysine-phosphate buffer without proteinase K treatment in order to preserve the integrity of the dendrites. After completion of in situ hybridizations, cells were washed with PBS and incubated in blocking buffer (4% goat serum in PBS 13) for 1 hr. Neurons were subsequently processed for immunofluorescence using standard methods (Aakalu et al., 2001). Images were obtained from 10 micron z-stacks (20 images) that were acquired with 2,048 x 2,048 pixel resolution. Both processed channels were merged using Adobe Photoshop.

3.1.6 Bicuculine treatment of primary neuronal culture

Rat primary hippocampal neurons were grown in 6 cm petri dishes at a density of 400K. At DIV28, neurons were treated with bicuculline (Tocris, 40 μM) or a water control for 12 hrs. Subsequently, cells were scraped using Trizol (Invitrogen) followed by RNA extraction.

3.1.7. RNase R treatment.

Mouse or rat brain DNase-treated total RNA (1ug) was incubated 15 min at 37oC with or without 3U/μg of RNaseR (Epicentre Bio-technologies). RNA was subsequently purified by phenol-chloroform extraction. Reverse transcription (RT) was performed using random hexamers and reverse transcriptase (SSIII, Invitrogen). Quantitative PCR (qPCR) was done using SYBR green master mix (Roche). For circRNA transcripts, one primer was designed to anneal at the circular junction whereas the other was within the circRNA transcript. For linear transcripts, both primers were designed to amplify the sequence that is not part of any circRNAs derived from the same gene locus.

3.1.8 qRT-PCR

Trizol extracted total RNA was treated with TURBO DNase (Ambion) following the manufacturer's protocol. Reverse transcription was performed using 1 ug of total RNA, random hexamers and Superscript III reverse transcriptase (Invitrogen) according to manufacturer's protocol. qPCR was carried out using SYBRGreen

Masrermix I (Roche) on LightCycler 480 (Roche) according to manufacturer's instructions. First stranded cDNA was diluted 1:100 and 5 l was used as template in a 20 ul qPCR reaction system: 4 ul H2O, 10 ul 2 x Master Mix, 0.5 ul Forward primer, 0.5 ul Reverse primer, 5 ul template. All assays were performed in triplicates. For expression quantification, the average fold change was calculated by normalization to *GAPDH*. For stability of circular RNA in RNAseR treatments, relative ratios were calculated by normalization to 5S rRNA and compared between treated and mock sample.

3.1.9 Primer design

For the circular RNA transcripts, primers were designed to anneal at the junction spanning part of its sequence. For the linear transcripts, primers were designed to anneal at the part of the sequence which does not produce any circle. qPCR primers are listed in Table 1.

Table. 1

(q)Rn_tr_Homer1_L_F	5'- ATA GCC GGG CAA ACA CT-3'
(q)Rn_tr_Homer1_L_R	5'- TCT CCT GCG ACT TCT CCT TT-3'
(q)Rn_tr_Gabrg3_L_F	5'- CTG CCA GAG CTT CTT CTG CT -3'
(q)Rn_tr_Gabrg3_L_R	5'- AGG AGT CCA GCT CAG AGA CG -3'
(q)Rn_tr_Tiam1_L_F	5'- GCC CAG GGC TCT TTA TTC TC -3'
(q)Rn_tr_Tiam1_L_R	5'- TGA ACG CTG TCC TGT CAC TC -3'
(q)Rn_tr_Homr1_C_F2	5'- TTG CCA TTT TCA CAT AGA ACA ACC TAT CT -3'
(q)Rn_tr_Homr1_C_R2	5'- CAT GCT TGC TGG TGG GTA CCC -3'
(q)Rn_tr_Gabrg3_C_F	5'- CCT TCT CTA GCT GAA TAC CAA ATT G -3'
(q)Rn_tr_Gabrg3_C_R	5'- ATC AAA CCC ACC ATG TTG CT -3'
(q)Rn_tr_Tiam1_C_F	5'- ACA GCA GCA AGC TTT ACA AAG A -3'
(q)Rn_tr_Tiam1_C_R	5'- CG TCC ACA GAA GAA AGC AA -3'
(q)Mm_dev_Dlgap1_L_F	5'- GGG CCA CTT AAG GTT TCA CA -3'
(q)Mm_dev_Dlgap1_L_R	5'- CCC GGG AAA TGT GAA CTA GA -3'
(q)Mm_dev_Myst4_L_F	5'- CAG ACA CAG AAG CAG GAC CA -3'
(q)Mm_dev_Myst4_L_R	5'- GGT CTC GGA GTC AAT TTC CA -3'
(q)Mm_dev_Ezh2_L_F	5'- CCC TGA AGT ATG TGG GCA TC -3'
(q)Mm_dev_Ezh2_L_R	5'- TGA AGC TAA GGC AGC TGT TTC -3'
(q)Mm_dev_Dlgap1_C_F	5'- CCC AGA AGA CAT GTC ATC TTG C -3'

(q)Mm_dev_Dlgap1_C_R	5'- CTG TGC TAC TCT GGG CTG TG -3'
(q)Mm_dev_Myst4_C_F	5'- TGC CCT TTG TAG AAA TAC TGA TAT TAA -3'
(q)Mm_dev_Myst4_C_R	5'- GCC TGC TTA AAA ACG TCC AG -3'
(q)Mm_dev_Ezh2_C_F	5'- GGG ACT AGG GAG AAT AAT CAT GG -3'
(q)Mm_dev_Ezh2_C_R	5'- TGA ACC TCT TGA GCT GTC TCA G -3'

3.1.10 In vitro transcription of Homer1 containing exons 2-5

Mouse cDNA was reverse transcribed and a fragment of Homer1 transcript containing exons 2-5 was amplified with gene-specific primers, with forward primer containing T7 promoter sequence. PCR product of 520 nt was transcribed in vitro with Biotin RNA Labeling Mix (Roche) and T7 RNA polymerase, followed by purification of the RNA with Ampure beads. The molecular weight of the RNA was checked by Agilent Bioanalyzer.

Hom1_T7_LC_F:
5'- GCT ACA TAA TAC GAC TCA CTA TAG GGC ATT TCC ACATAG GGAGCA ACC TAT C-3'

Hom1_LC_R:
5'- GCA ATG CAT TCT GAG TTG GCTC-3'

as _Hom1_F (LL):
5′- GGAGCAACCTATCTTCAGCACTCG-3′

as T7_Hom1_R (LL):
5′- GCT ACA TAA TAC GAC TCA CTA TAG GGCTA TGT GGA AAT GGC AAT GCA TTCTGAG-3′

3.1.11 Biotinylated RNA Pull-Down

The RNA pull-down assay was performed as previously described (Tsai et al., 2010). In brief, in vitro transcribed biotynilated RNA was folded in RNA structure buffer and the RNA was folded by adding an equal volume of RNA structure buffer (20 mM Tris

[pH 7.0], 0.2 M KCl, and 20 mM MgCl2), heated to 70C for 5 min, and slowly cooled to room temperature in order to allow proper secondary structure formation. 50 pmol of IVT transcript was adsorbed onto streptavidin magnetic beads (Streptavidin MyC1, Invitrogene). Mice (age 4–6 weeks old) were sacrificed, and brains were harvested and homogenized using RIP buffer (150 mM KCl, 25 mM Tris [pH 7.4], 0.5 mM DTT, 0.5% NP-40, and complete protease inhibitors) with a Dounce homogenizer. Homogenate was resuspended with syringe and centrifuged at 14 000 *g* for 10 min at 4 °C. RNA-loaded beads were incubated with pre cleared cell lysate at 4°C for 4 hr. Next, beads and washed five times in RIP buffer. Half of the beads were incubated and eluted in Laemmli buffer and run on SDS-PAGE gels for western blot . The other half was eluted in 8M urea and prepared for mass spectrometry analysis. The dilutions for western blot of the following primary antibodies are as follows: goat anti-FMRP (Santa Cruz Biotechnology, 1:200) and mouse anti-hnRNPA2/B1 (Sigma-Aldrich, 1:1000), snit-beta Tubulin, Sigma, 1:5000).

3.1.13 In-solution digestion for LC-MC analysis

Proteins eluted form beads were reduced in DTT 2mM for 30 minutes at 25 °C. Free cysteines were alkylated in 11 mM iodoacetamide for 20 minutes at room temperature in the darkness. LysC digestion was performed by adding LysC (Wako) in a ratio 1:40 (w/w) to the sample and incubating it for 18 hours with gentle shaking at 30 °C. After LysC digestion, the samples were diluted 3 times with 50 mM ammonium bicarbonate solution, 7 µl of immobilized trypsin (Applied Biosystems) were added and samples were incubated 4 hours with rotation at 30 °C. Digestion was stopped by acidification with 10 ul of trifluoroacetic acid and trypsin beads were removed by centrifugation. 15 micrograms of digest were desalted on STAGE Tips, dried and reconstituted to 25 µl of 0.5 % acetic acid in water.

3.1.12 RNA Immunoprecipitation

For RIP assay, 5 µg of anti-FMRP was used (03-108 Merck, Millipore) Briefly, after homogenisation in complete RIP Lysis Buffer, lysate was centrifuged at 14,000 rpm for 10 minutes at 4°C. 100 µL of the supernatant was added to each beads-antibody complex in RIP Buffer up to the final volume of 1.0 mL. Additional 10 µL of the supernatant, representing '10% input' was used for RT-qPCR and RNA quality assessment. The other 10 µL of the supernatant of RIP lysate was used to test the expression of RNA- binding protein of interest by WB. After overnight rotation at 4°C beads were washed six times with 500 µL of cold RIP Wash Buffer. The proteins were eluted off the beads by re-suspending the beads in 1X SDS-PAGE loading buffer followed by heating at 95°C. The beads were centrifuged down and the supernatant directly applied on SDS-PAGE. Immunoprecipitated protein/RNA complexes were digested with ProteinaseK buffer at 55C with constant shaking for 30 min, followed by phenol/chloroform RNA purification.

3.2. Computational methods

3.2.1 Quantification of Transcript Expression

The paired-end or single 120bp reads, depending on the sample were mapped to the mouse Ensemble database (GRCm38) using the read alignment software bwa (Li and Durbin, 2009) without seeding and allowing for one mismatch, after removing the adapter sequences from the read ends using FAR (http://sourceforge.net/projects/theflexibleadap/). To quantify transcript expression for all gene loci, we calculated reads per kilobase of transcript sequence per million mapped reads (RPKM) (Pepke *et al*., 2009), dividing by the total amount of kilobases of all transcripts originating from a gene locus, by summing up the reads of all isoforms. Non uniquely mapped reads

were discarded. If no reads were mapped to a locus, a pseudocount of one was added to the locus.

3.2.2 Total transcriptional output (TTO)

Total Transcriptional Output (TTO) estimation

After removing the Illumina sequencing adaptor at 3‟ end, the reads were aligned to the mouse (mm9) or rat (rn5.0) genome reference sequences using Tophat2, allowing up to six mismatches. Cufflinks (v2.21) (Roberts A. et al., 2011) was then used to estimate the total transcriptional output based on Ensembl gene annotation for mouse (mm9, version67) or rat (rno5.0, version72). Genes annotated as “protein-coding” or “lincRNA” were retained for further analysis. To compare gene expression between two samples, we converted the FPKM (Fragments per kilobase per million) to TPM (Transcripts per million) using the following formula: TPM = FPKM * 1,000,000 / (sum_of_FPKM).

3.2.3 Circular RNA identification and quantification

For each sample, the unmapped reads were aligned to the respective genome reference sequences by BWA [34] in local mode (with parameters: - mem -k16). Partial alignments of segments within a single read that mapped to i) regions on the same chromosome and no more than 1Mb away from each other ii) on the same strand iii) but in reverse order, were retained as candidates supporting head-to-tail junction. The strength of potential splicing sites supported by these candidate head-to-tail junction reads was then estimated using MaxEntScan (Yeo et al., 2004). The exact junction site was determined by selecting the donor and accepter sites with the highest

splicing strength score. Candidate circRNAs were reported if the head-to-tail junction was supported by at least two reads and the splicing score was greater than or equal to 10. To estimate the expression of circRNA, we re-aligned all the unmapped reads to the circular candidates. As for most of the circRNAs there is no direct evidence for their exact sequence, we filled in the sequence using existing exon annotation. Sequence at the 5‟ end was concatenated to the 3‟ end to form circular junctions. Reads that mapped to the junction (with an overhand of at least 5nt) were counted for each candidate. TPM (Transcripts Per Million) was calculated for each circRNA candidate, where the effective length was calculated as: (sequencing length – 2 * 6). The analysis pipeline with a detailed description is publicly available at (https://code.google.com/p/acfs/).

3.2.4 Mass spectrometry data processing and analysis

Raw data were analyzed using the MaxQuant proteomics pipeline (v1.2.2.5) and the built in the Andromeda search engine (Cox, Neuhauser et al. 2011) with the International Protein Index Human version 3.71 database, Carbamidomethylation of cysteines was chosen as fixed modification, oxidation of methionine and acetylation of N-terminus were chosen as variable modifications. The search engine peptide assignments were filtered at 1% FDR and the feature match between runs was not enabled; other parameters were left as default.

4. RESULTS

4.1 Synaptosomes isolation provides distinct subcellular fractionation and significant enrichment of synaptic region

In order to perform gene expression profiling of coding and functional non-coding RNAs in synaptic region, we purified synaptosomes, i.e. detached nerve terminals enclosed in membraneous vesicles, from the pool of 4 to 6 weeks old mouse brains, using biochemical fractionation on Percoll gradients (Dunkley et al., 2008). We modified the original protocol from Dunkley et al., 2008, since it was developed for downstream analysis of protein, yielding RNA of insufficient quality for high-throughput sequencing. The protocol was optimized for RNA analysis by introducing a change in the reagent used for establishing discontinuous sucrose gradients for separation of synaptosomes. Instead of separation on gradients containing polyvinylpyrrolidone (PVP) coated Percoll particles, synaptosmes were separated on gradients containing silan coated Percoll particles. This change in the protocol dramatically improved the quality of RNA, which is suitable for sequencing (Figure 9).

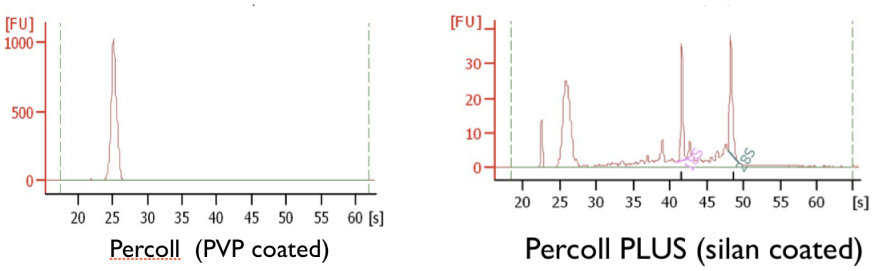

Figure 9. Total RNA isolated from synaptosomes on Percoll and Percoll Plus reagent (GE Healthcare). The integrity of total RNA isolated from the samples was analyzed using an Agilent 2100 Bioanalyzer. The ratio for18:28 rRNA is very good for total RNA isolated on Percoll Plus gradients(silan coated) gradient and very poor for RNA isolated on Percoll (pvp coated) gradient.

Briefly, pool of 3 adult mouse brains were sheared in isotonic medium with Douncer homogeniser. Detached nerve terminal membranes enclosed in synaptosomes were isolated using medium speed centrifuge while maintaining isotonic condition. After separation on sucrose/Percoll gradients, five major fractions were generated. Compared to other layers containing more membraneous and myelin vesicles, fraction 4 (F4) represented the most pure synaptosomes (Dunkley et al., 2008) and were used in subsequent gene expression profiling experiments (Figure 10A).

The enrichment of synaptic proteins and depletion of glial proteins in synaptosomal fraction was validated by Western blot (Figure 10B). AMPA receptor subunit (GluR4) is enriched in synaptosomes compared to whole brain lysate, while glial fibrillary marker protein (GFAP) is substantially reduced, indicates that non-synaptic glial contaminants were by large depleted from the sample. Furthermore, based on the GM130, Golgi complex marker, we could demonstrate the absence of cell body contaminations. Finally, we could demonstrate the integrity of synaptosomes with electron microscopy (EM), (Figure 10C), which showed the presence of enclosed vesicles withe the parts of presynaptic membrane attached In summary, the validation experiments suggested that F4 fraction was sufficiently pure for the downstream analysis.

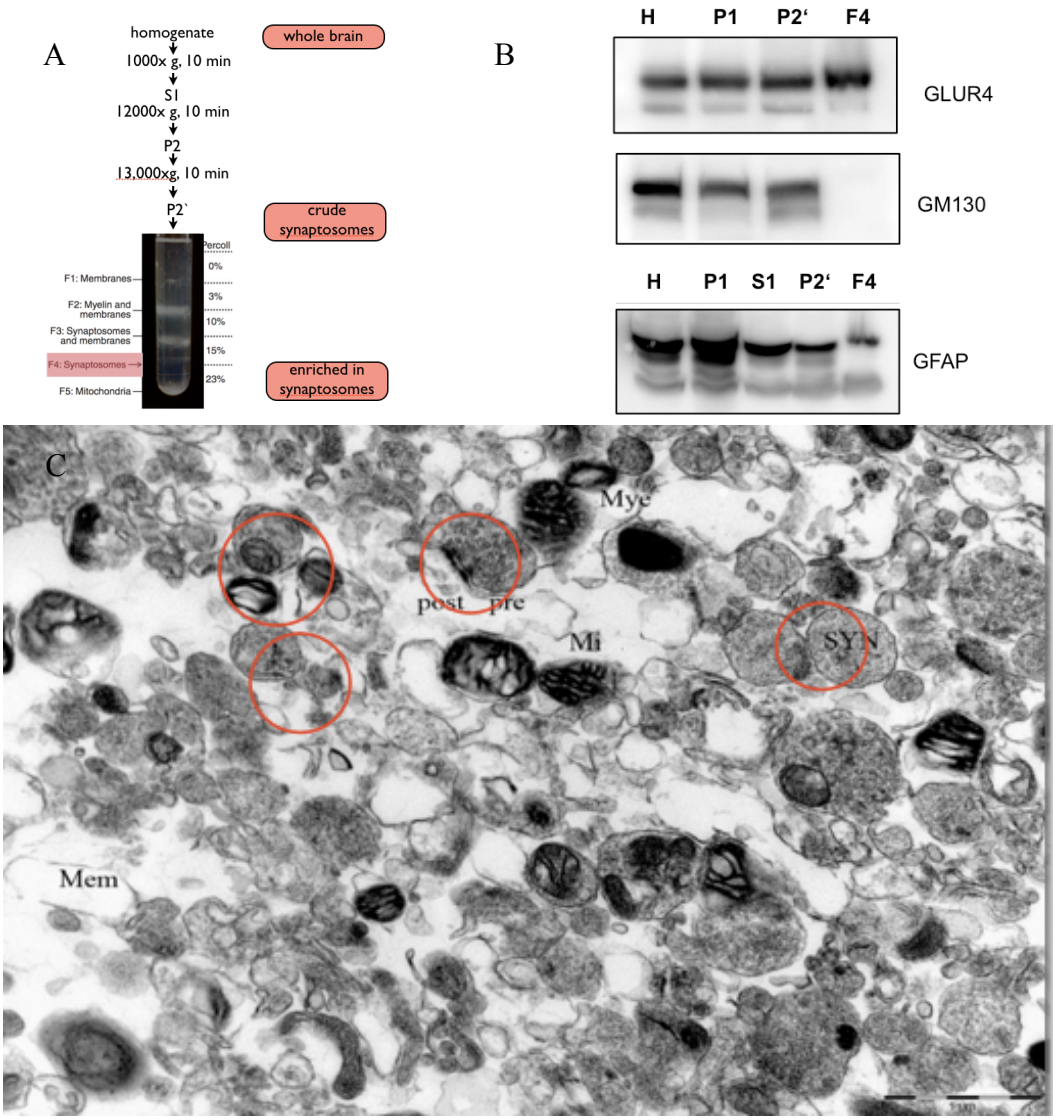

Figure 10. Synaptosomes. (A) Shematic representation of synaptosomes isolation. **(B)** Enrichment of synaptosomes was validated by Western blot analysis of protein extracts derived from different centrifugation fractions; whole brain (H), centrifugation pellet (P1) and (P2) and synaptosmes (F4). Whereas postsynaptic glutamate receptor subunit GLUR4 is enriched in synaptosomes, cytoplasmic Golgi marker GM100 is completely absent and glial fibrillary acid protein GFAP is substantially decreased from synaptosomes. **(C)**Electron microgram of a synaptosome fraction showing predominantly larger diameter synaptosomes (Syn) denoted in red, synaptic vesicles, relatively few mitochondria (Mi) and numerous membranes (Mem) and membranous vesicles.

4.2 Synaptosomes isolation protocol allows reproducible quantification of transcripts by mRNA-seq

To determine the reproducibility of RNA profiling of synaptosomes resulting from a multi-step protocol, we sequenced polyA-RNA isolated from the mouse whole brain synaptosomes and mouse whole brain lysate in biological duplicates. In each of four samples, we obtained about 30 million reads with 74% to 97% of reads uniquely mapped to Ensemble, a reference transcript database (Table 1). Since the fraction of mitochondria within synaptosome sample (F4) is estimated to be around 50%) and as such would influence the transcript quantification, we excluded the reads mapped to mitochondrial mRNA transcripts. After that, we detect 24, 187 transcripts in the whole brain and 21, 616 transcripts in the whole brain synaptosomes with the expression level defined as reads per kilobase of transcript per million of mapped reads (RPKM), see Computational Analyses. Next, we compared the reproducibility of synaptosome RNA profiling. As expected, the technical replicates showed the best correlation (r=0.989, Figure 11A). Biological replicates for independently isolated synaptosomes showed an excellent correlation (Figure 11C) with the correlation coefficient, (r=0.949), just slightly lower than that for two biological replicates of the whole brain sample (r=0.967), Figure 11B), which does not go through a multi–step isolation procedure.

TABLE 1. Sequencing statistics	whole brain		enriched in synaptosomes	
# raw reads	31, 022,433	31, 575,326	30, 176,478	31, 641,140
% mapped to genome	73.86%	66.82%	82.94%	82.57%
# genes mapped to Ensemble	24, 187		21, 616	

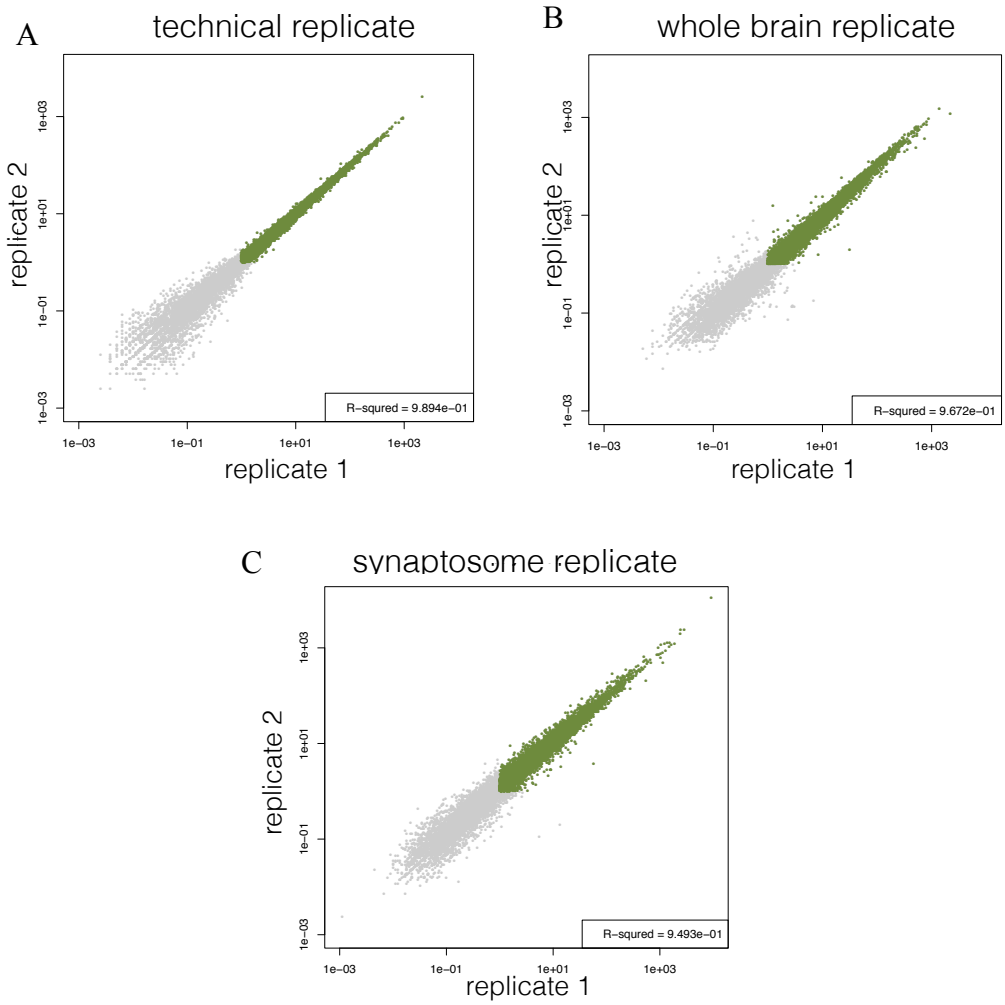

Figure 11. Reproducibility of synaptosome profiling. Scatter plots showing expression levels in RPKM on log2 scale for (A) technical replicates (B) whole brain replicates (C) synaptosomes replicates. Each gene is represented by a dot, a colour indicates transcripts below the expression level threshold, RPKM<1 (grey) and 13,303 transcripts with RPKM>1 (green). Technical replicates show the best correlation (r=0.989). Biological replicates for independently isolated synaptosomes (r=0.949), (C) show very good and comparable reproducibility to two biological replicates of the whole brain samples (r=0.967), which does not go through the multi–step process.

4.3 Analysis of differential gene expression between hippocampal synaptosomes and whole hippocampus

After demonstrating the high reproducibility between the biological replicates of synaptosome preparation, we went on to identify the full population of mRNAs present in synaptic region of mouse hippocampus, a brain region involved in memory, cognition, mood regulation and stress response, as well as one of the brain regions most frequently implicated in mental illness. (De Carolis et al., 2010). We profiled ribosomal RNA (rRNA) depleted RNA from synaptosomes isolated from the pool of five hippocampi of the two weeks old mice. In total, we obtained 30 x 106 Single-end 120 bp sequencing reads, of which 85 % mapped uniquely to Ensebmle . The observed range of gene expression for 16, 736 protein coding genes spanned six orders of magnitude, from 10(-3) to 10(3) RPKM. Among them, 11, 303 protein coding genes with the expression value RPKM>1. We set our filter criteria based on the assumption that 1–5 r.p.k.m. approximates to 1 copy per cell (Kellis et al., 2014), we only include these 11,303 genes in further analysis. To identify significantly overrepresented gene families and protein functions in this data set compared to a background gene set (all Ensembl database genes), we used DAVID Functional Annotation tool for gene ontology (GO) enrichment analysis. Proteins encoded by detected transcripts were enriched in categories associated with neuronal function, e.g. genes associated with vesicle mediated transport, neuron projection development, axonogenesis, synaptic transmission, ion homeostasis etc. (Figure 12).

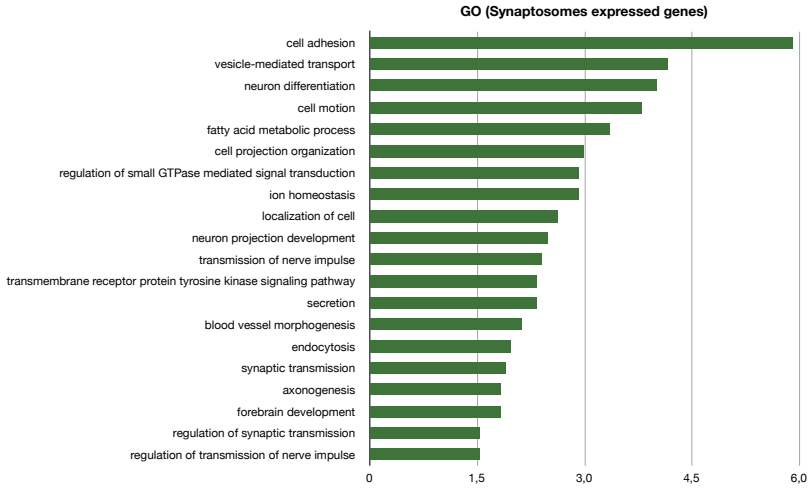

Figure 12. Gene Ontology Analysis (GO) of transcripts detected in hippocampal synaptosomes. Bar graph illustrating some transcript families from (GO) that are significantly overrepresented in our sample.

Further, to search for transcripts that are enriched in neuronal compartments, we also profiled the RNAs from the whole hippocampus where we detected 17, 493 transcripts, 11, 917 of them with the expression value RPKM>1 and performed a differential gene expression analysis between synaptosomes and the whole brain. As transcription occurs in the nucleus followed by export of the mRNA to the cytoplasm, all neuronal transcripts, regardless of their ultimate destination, reside in the cell body for some period of time. Thus, it is expected that, assuming perfect detection, all dendritic transcripts should also be discovered in the cell body. Nevertheless, we reasoned the transcripts that are ≥2 fold enriched in synaptosomes compared to the whole hippocampus could not result from passive transcript diffusion but rather from active transport. In total, 1,446 protein coding genes, 590 with the expression value RPKM>1 were found to be ≥2 fold enriched in synaptosomes compared to the whole brain (Figure 13A). Again using DAVID GO enrichment analysis above, GO terms for these 590 genes were enriched in terms involved in aspects of synaptic function; presynaptic membrane, axon part, postsynaptic density, dendrite, ribosome, synapse

part and mitochondrial function, demonstrating these transcripts are probably transported and locally translated rather than randomly diffused.

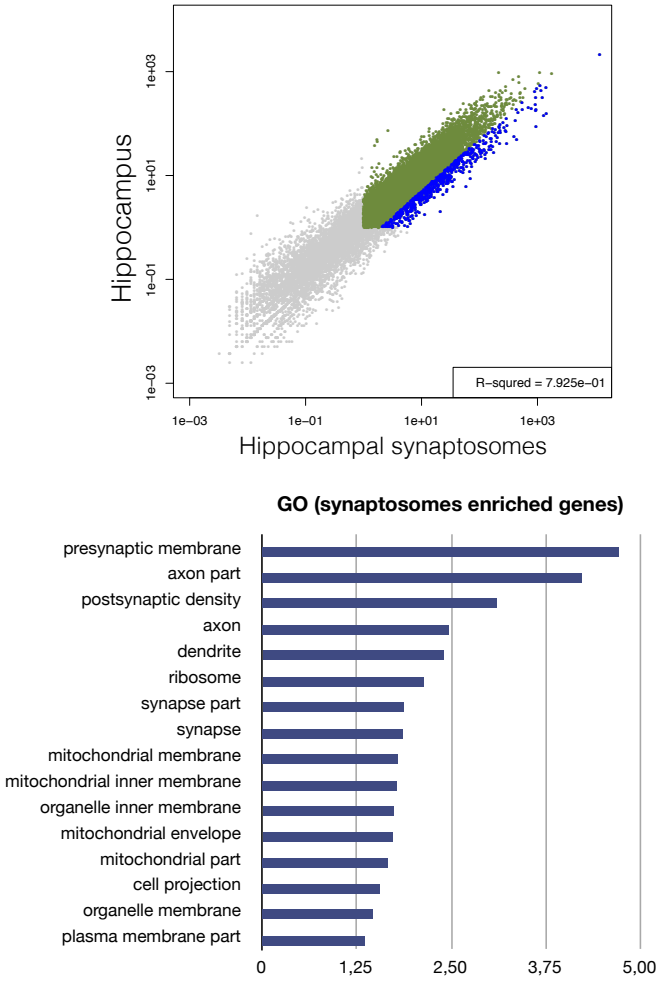

Figure 13. **Enrichment analysis for poly(A) RNA transcripts in hippocampal synaptosomes. (A)**Differential gene expression in hippocampal synaptosomes vs whole hippocampus. Scatter plots showing expression levels in RPKM on log2 transformed scale, synaptosomes (x-axis) and whole hippocampus (y-axis). Transcripts below the expression level threshold, RPKM<1 (grey), 13,303 transcripts with RPKM>1 and 590 transcripts >2 fold enriched in synaptosomes (blue). **(B)** Bar graph illustrating some transcript families from (GO) that are significantly overrepresented among >2 fold enriched transcripts in synaptosome sample.

4. 4 Extended repertoire of transcription factors enriched in synaptosomes

After demonstrating the enrichment of synaptic-function relevant transcripts in synaptosome, we sought to search for synaptosome enriched transcripts previously non-related to synaptic function. Here we focused on transcription factors (TFs), critical regulators of gene expression, thought to be primarily restricted to the nucleus and surrounding cell soma. However, local translation and translocation of several TF from postsynaptic sites to the nucleus is known to be critical for key neuronal processes like circadian rhythms, long- term memory and neuronal survival (Deisseroth, 2003). Among them CREB, CEBP-1, STAT3, SMADs) has been linked to axonal retrograde signalling (reviewed in Deglincerti and Jaffrey, 2012) and were shown to function as a part of a synapse-to-nucleus signalling cascade.

To systematically analyse the differential expression of TF in hippocampal synaptosomes vs whole hippocampus, we extracted a set of 1651 TF and TF related genes from Swiss-Prot Protein database. As expected, most of TFs were strongly depleted from synaptosomes or showed no enrichment compared to the whole hippocampus, including the known literature examples CREB-1, CEBP-1, STAT3, and SMADs, which are known to have a synaptic function (Figure 14A). Interestingly, we identified 45 TF and TF- associated genes with ≥2 fold enrichment in synaptosomes (Table 2). The enriched genes spanned the whole range of expression and therefore it is unlikely that such enrichment results from normalization artefact. Among the 45 genes, we detected a handful of TF which function during normal embryonic development and were previously not related to synaptic function. For instance, members of Sox family transcription factors (Sox2, Sox6 and Sox21) are well-established regulators of cell fate decisions during development, and more recently recognised as regulators of adult tissue homeostasis and regeneration (Sarkar

et al., 2013), as well as ZEB family of zinc finger transcription factors (Zeb1 and Zeb2), known to be essential players in epithelial to mesenchymal transition (EMT), (Vandewalle et al., 2009).

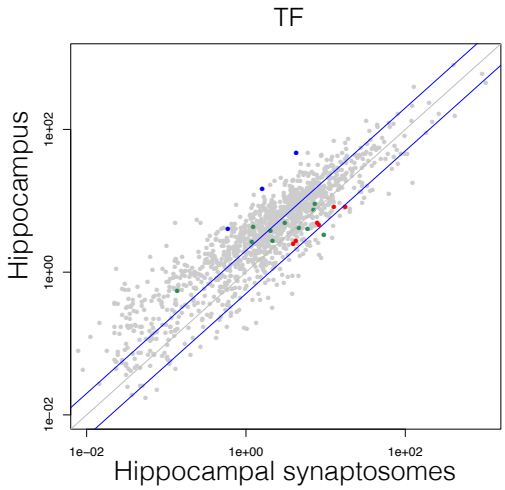

Mmp14	2,06	Lhx2	2,36	Heyl	2,82
Sox6	2,08	Ntrk2	2,4	Epas1	2,89
Cat	2,08	Zeb1	2,4	Tsc22d4	2,92
Dazap2	2,11	Taf13	2,41	Pbxip1	2,98
Aldh2	2,16	Ctdsp1	2,42	Fgf1	3,0
Sox9	2,19	Hsd11b1	2,45	Wwtr1	3,02
Mt3	2,21	Sall1	2,46	Rfx4	3,08
Yap1	2,24	Nfe2l2	2,50	Nr2e1	3,1
Foxo4	2,27	Irf5	2,51	Hipk2	3,24
Etv4	2,27	Tmem173	2,51	Emx2	3,62
Clu	2,32	Mdk	2,56	Tgfb1	4,08
Sox21	2,32	Prkd1	2,61	Tgfbr1	4,28
Tcf7l1	2,33	Smo	2,71	Itgb5	4,35
Ppap2b	2,34	Hopx	2,82	Inpp5d	5,23
Cebpa	2,36	Heyl	2,82	Csf1r	6,34

Figure 14. **Enrichment analysis for transcripts coding for TF in hippocampal synaptosomes. (A)** Differential expression of transcripts coding for TF in hippocampal synaptosomes vs whole hippocampus. Scatter plots showing expression levels in RPKM on log2 transformed scale for 1651 TF and TF-related genes, synaptosomes (x-axis) and whole hippocampus (y-axis). Known literature examples of TF locally translated at the synapse (blue), candidates for ISH validation (red). **(B)** List of mRNAs encoding TF and TF related genes that displayed an at least two-fold change in expression between synaptosomes and whole hippocampus. Candidates for ISH validation in red (Sox9, Foxo4, Lhx2 and Zeb1, second column-fold enrichment.

To investigate the subcellular localization of TFs identified in our screen, we performed in situ hybridization (ISH) in rat hippocampal neurons at 18 days in vitro (DIV), (Figure 15).We chose for validation well studied TFs that were moderately to highly expressed (RPKM>1) and ≥2 fold enriched in synaptosomes, i.e. Zeb-1, Sox9, Lhx2 and Foxo4. Three out of four (Zeb-1, Sox9, and Foxo4) were readily detected in cultured hippocampal neurons by using Panomics branching probes with signals (green puncta) extending well into neuronal processes (that were identified as dendrites and axons by co-staining for dendritic/and/or/axonal marker MAP2), while Lhx2 could not be detected. Taken together, our sequencing and ISH data show that a specific subset of TF is enriched in the synaptodendritic compartment of murine neuron.

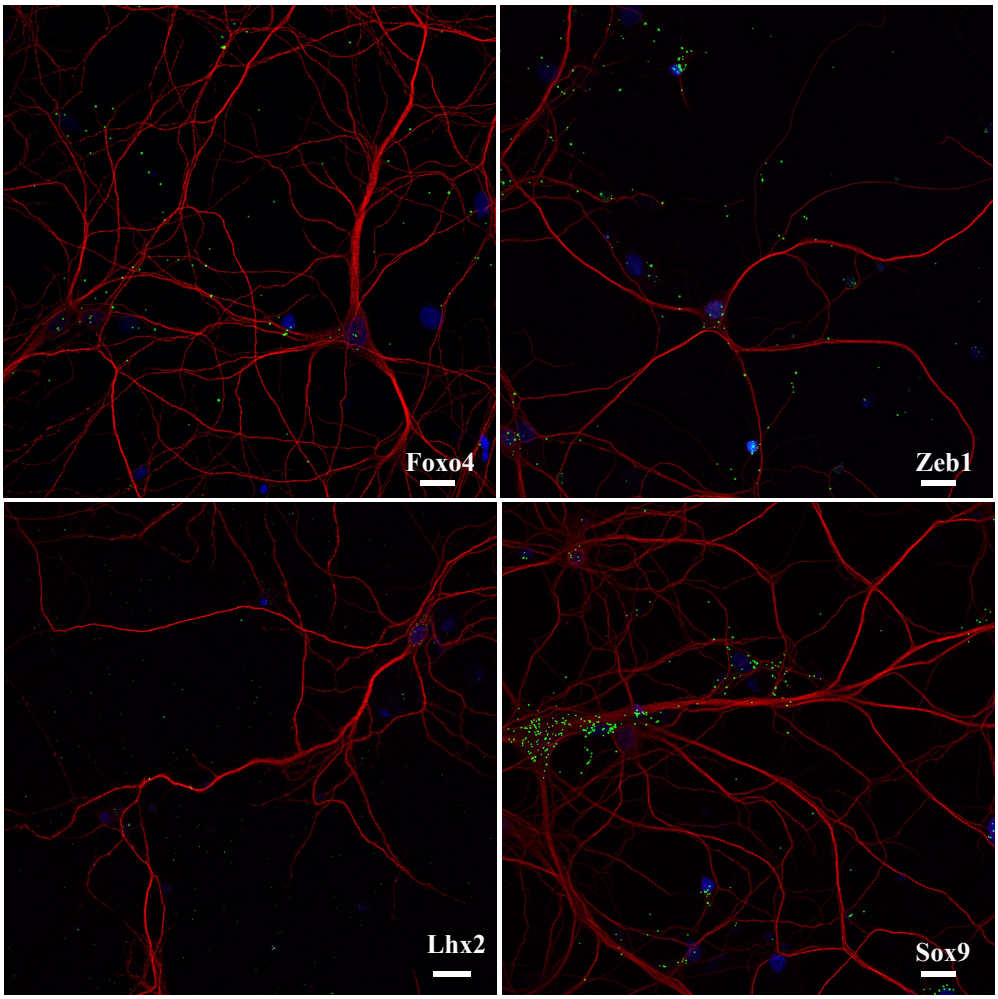

Figure 15. Detection of TF transcripts in the dendrites of cultured rat hippocampal neurons. Fluorescent in situ hybridization (FISH) signal in cultured hippocampal neurons (DIV 21) showing the presence of *Foxo4, Sox9 and Zeb1* mRNA molecules (green puncta) within the cell body and dendritic arbor, while *Lhx2* transcript could not be detected. The neuron was immunostained with an antibody to MAP2 (green) to generate a mask that outlines the dendrites (red). Scale bar = 20 um.

4.5 Comparison with the previous data, hippocampal transcriptome from rat neuropil

To asses the prevalence of mRNAs localised to neuronal synapse, we also compared our hippocampal synaptosomes data set with the most recently published neuropil transcriptome dataset (Cajigas et al., 2012) the one reporting so far the highest number of transcripts localised to synaptic region. Compared with that study, we used a different sequencing technology platform (Illumina) which provides higher sensitivity in RNA detection than the one (454) used in Cajigas et al. In our data set, we chose expression level of RPKM>1 as a threshold value for inclusion in the final data set, yielding 11, 303 unique mRNAs from mouse hippocampal synaptosomes. In comparison, 8, 379 mRNAs were identified in that rat neuropil data set (Cajigas et al.). We found substantial overlap between two data sets. 6, 448 out of 8, 379 rat neuropil unique mRNAs (76,9%) were readily detected in mouse hippocampal synaptosomes (Figure 16A). The remaining 1, 931 genes were detected within the group of genes with the expression level lower than RPKM>1 and therefore excluded from the final dataset. (Figure 16C). In contrast, the expression of 2, 924 mRNAs detected in mouse hippocampal synaptosomes but not present in rat neuropil spanned the expression range of 3 orders of magnitude (Figure 1C), similar to mRNAs detected in both datasets.

To exclude potential contaminants, we further refined the list of transcripts of dendritic and/or axonal origin by applying the same filter criteria as in Cajigas et al., 2012. Based on previously published data sets, a union of all transcripts to be filtered contained 9, 601 genes. It includes data on transcripts enriched in astrocytes and oligodendrocytes (Cahoy et al., 2008; Okaty et al., 2011), interneuron- enriched transcripts (Klausberger and Somogyi, 2008; Okaty et al., 2011; Sugino et al., 2006), in situ hybridization data (http://mouse.brain-map.org/) and mRNAs enriched in blood vessels (Daneman et al., 2010) and mitochondirion (http://mitominer.mrc-mbu.cam.ac. uk/release-1.1) and transcritps that code for nuclear proteins. Following subtraction, our hippocampal synaptosomes dataset resulted in 5, 087 transcripts compared to 2, 453 transcripts detected in rat neuropil. (Figure 16B). The overlap between two filtered data sets was even higher, 2, 229 out of 2, 487 unique mRNAs form rat neuropil (89,6%) were readily detected in mouse hippocampal synaptosomes. (Figure 16B). The remaining 258 genes were detected within the group of genes with the expression level of RPKM<1 and therefore excluded from the final dataset. (Figure 16D). Further, the expression of 2, 634 genes detected in hippocampal synaptosomes but not present in rat neuropil spanned the expression range similar to gene detected in both datasets. (Figure 16D).

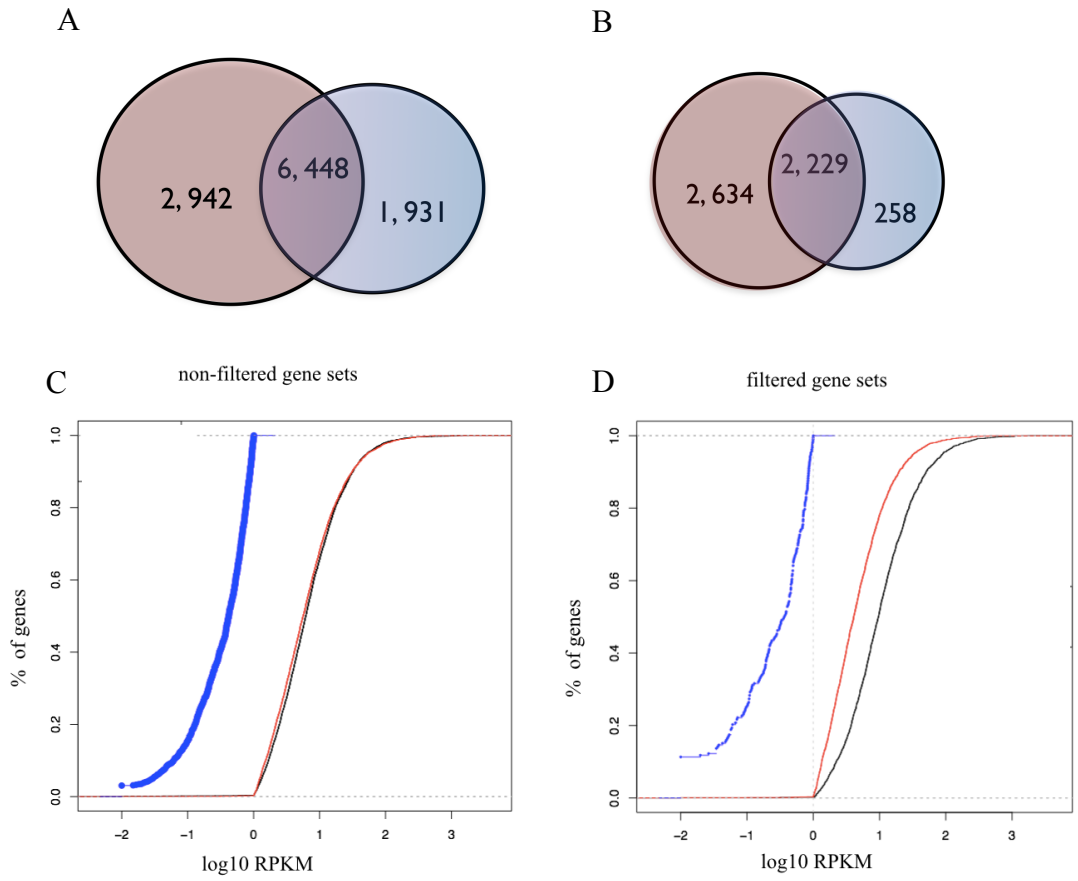

Figure 16. Comparison of hippocampal synaptosomes with transcriptome from rat neuropil (Cajigas et al., 2012). **(A)** Venn diagram showing the overlap between our mouse hippocampal synaptosomes set (red) and rat neuropil set (blue), (Cajigas et al., 2012). **(B)** Venn diagram showing the overlap between our filtered set (red) and filtered set of rat neural mRNAs (blue),(Cajigas et al., 2012). **(C)** Expression level of transcripts detected in our sample but not in Cajigas et al., (red) and transcripts detected only in Cajigas et al. but not in our dataset (blue). Expression as log2 transformed RPKM value on x-axis. **(D)** Expression level of filtered sets of transcripts detected in our sample but not in Cajigas et al., (red) and transcripts detected only in Cajigas et al. but not in our dataset (blue). Expression as log2 transformed RPKM value on x-axis.

4.6 Profiling of circular RNAs across tissues reveals enrichment in brain

The expression of circular RNAs was quantitated using RNA- sequencing of rRNA depleted samples across different mouse tissues, including brain, liver, lung, heart and testis. In each tissue, we obtained a minimum of 27 x 106 reads (brain) and a maximum of 47 x 106 reads (testis) with mappable reads ranging from 79.0 to 97.2 %, depending on the tissue. The expression of cRNAs was determined by searching for reads that spanned the 5' and 3' ends of exon(s) in reverse order from the same linear transcript (Table 3).

Table 3. Sequencing statistics for circular RNAs

	Brain	Liver	Hung	Heart	Testis
Total No. reads	27224503	29083895	34189720	39368194	47388210
No. reads mapped to genome	21500556	28030600	32800368	38176921	46050976
No. reads mapped to Ensembl protein coding genes	11224201	17098786	12051503	21638890	27390819
No. of Ensembl protein coding genes expressed (RPKM >= 1)	11776	9342	11253	10048	11114
No. circular junction reads	16840	1587	2383	3998	36733
No. cRNA species	4143	859	1318	1702	5207
No. cRNA-hosting Ensembl protein coding genes	1982	637	919	1074	2145

The percentage of circular junction reads from all the reads mapped on Ensembl protein coding genes was highest in brain (0.15%), followed by testis (0.13%), lung (0.02%), heart (0.018%), and liver (0.009%), (Figure 17A). Further, the percentage of genes that produced cRNAs from all the expressed genes (RPKM>=1) was highest in testis (19%), followed closely by brain (17%) and much less in heart (10%), lung (8%) and liver (7%), (Figure 17B). Highest percentage of genes that produced cRNAs in testis and brain is not surprising since both tissues have complex transcriptional landscapes and gene expression profiles are most similar to each other, compared with

other tissues (Guo et al.). Two factors contributed to high abundance of circular RNAs in brain. First, many linear genes that produce circular RNAs are expressed in brain but not in other tissues, as shown for brain and liver (Figure 17C). Second, on average, when a linear gene is expressed in brain as well as other tissue(s), more circular RNAs are produced from the linear transcript in brain. We calculated the abundance of circular RNAs for each locus that produce cRNAs in both brain and liver (RPKM>1), represented by RPKM based on circular junction reads mapped to Ensembl protein coding genes, as a fraction of total transcriptional output (TTO) from the same locus, represented by RPKM based on all the reads mapped to the same gene locus. As shown in Figure 17D, by large, the fraction of circular RNAs for a given locus is higher in the brain than in the liver.

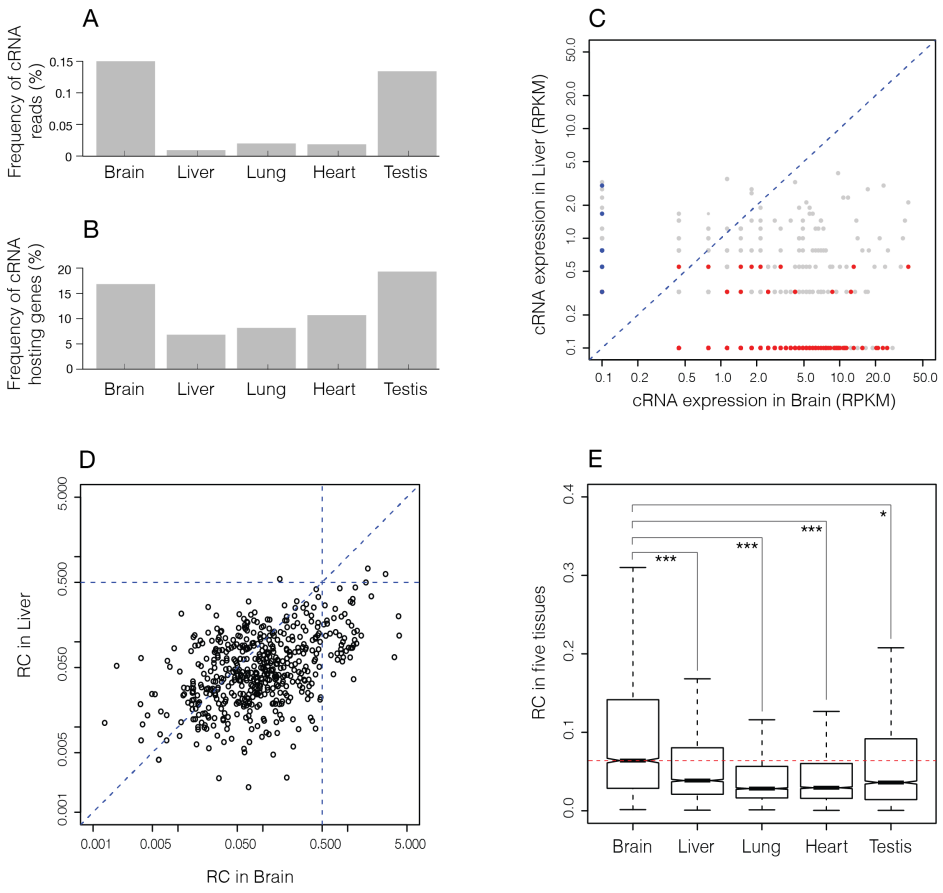

Figure 17. Profiling of circular RNAs across tissues reveals enrichment in brain. (A) The percentage of circular junction reads from all the reads mapped on Ensembl protein coding genes shown for different tissues, with the highest value (0.15%) in brain, followed by testis (0.13%). **(B)** The percentage of genes that produced cRNAs from all the expressed genes (RPKM>=1) was shown across different tissues, with the highest value (19%) in testis, followed closely by brain (17%). **(C)** The abundance (RPKM, reads per kilo base circular junction per million mapped reads to Ensembl protein coding genes) of circular RNAs was compared between brain (X-axis) and liver (Y-axis). Each dot represents one distinct gene locus. The value on X/Y axis represent the abundance of all circular RNAs derived from the gene locus. The linear genes that were not expressed in brain or liver (RPKM<1) are marked in red or blue respectively. Dots in grey were the genes expressed in both tissues. **(D)** For the genes that produce cRNAs in both brain and liver, the relative abundance of cRNAs versus the total transcriptional output (hereafter termed TTO) derived from the same gene locus was compared between brain (X axis) and liver (Y axis). On average, the transcriptional contribution of circular RNAs is higher in brain than that in liver. **(E)** On average, the relative contribution of circular RNAs is higher in brain than that in liver. E. The relative contribution of circular RNAs is significantly higher in brain than that of all other tissues (Student T-test. *** for p-value < 2.2E-16 and * for p-value < 0.05).

To validate the presence of candidate cRNAs we show by qPCR the insensitivity of 4 circRNA candidates to digestion with RNase R, an exonuclease that degrades linear RNA molecules (Figure 18).

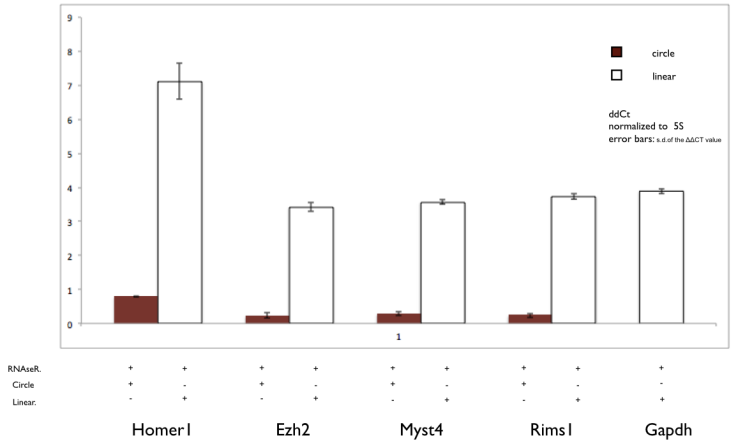

Figure 18. CircRNAs are resistant to RNase R treatment. (qPCR; error bars indicate standard deviation).

4.7 Synaptic localization of brain expressed circular RNAs

We conducted a Gene ontology enrichment analysis of the genes that give rise to brain-expressed cRNAs and found that functional groups related to synaptic function were significantly overrepresented (Figure 19A). For example, the groups synapse, synapse part, cell junction, postsynaptic membrane, presynaptic membrane and postsynaptic density were amongst the ten most significantly enriched functional categories in the neuronal cRNA population.

To examine whether cRNAs are enriched in synaptic tissue we sequenced a rRNA depleted mouse hippocampal synaptosome sample. The abundance of circular RNAs was compared between synaptosomes and a whole hippocampal homogenate. In total we detected 4, 143 candidate cRNAs from 1, 982 genes supported by 16, 840 reads in samples which in total expressed 11, 776 protein coding genes. We found that most cRNAs are indeed enriched in synaptic fraction examined (Figure 19B).

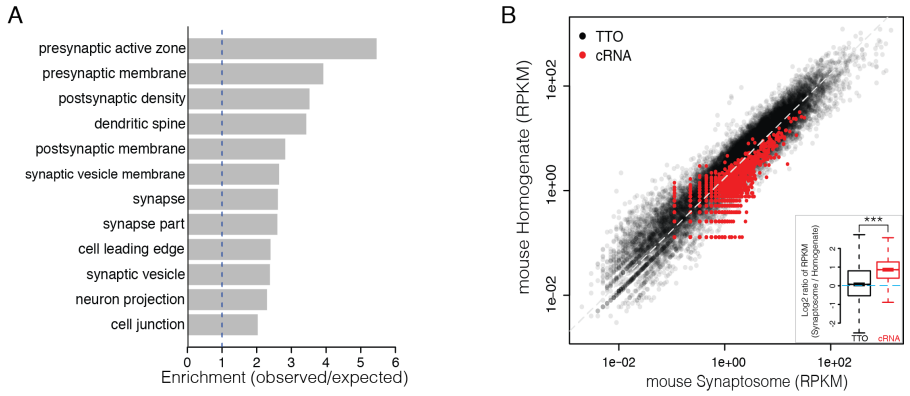

Figure 19. Synaptic localization of brain expressed circular RNAs. A. Gene ontology enrichment analysis of the genes producing brain expressed circular RNAs. Functional groups related to synaptic function are overrepresented in the genes producing brain expressed circular RNAs. B. Circular RNAs are of higher abundance (measured by RPKM) in mouse hippocampal synaptosomes (X-axis) compared to that in hippocampal homogenates (Y-axis). Each red dot represents one circular RNA, and each dark dot represents one protein coding gene.

4.8 Expression of circular RNAs in brain during development

To determine whether the expression of cRNAs is developmentally regulated, we profiled the cRNA population in the hippocampus over several developmental stages: embryonic brain (E18), early postnatal brain (P1), postnatal brain at the beginning of synapse formation (P10) and late postnatal brain following the establishment of mature neural circuits (P30). As shown in Figure 20A, there was a clear shift in the cRNA expression pattern associated with the synaptogenesis and maturation of neural circuits. Further, many cRNAs change their expression independent of their hosting mRNAs during the synatogenesis, although as a group, the expression of cRNAs correlate modestly with the total transcriptional output (TTO) of their gene loci (Figure 20B). Such difference between cRNA and its linear host gene in expression pattern across development might implicate differential regulation and function. We chose three genes with different expression patterns to validate their linear and cRNA expression changes across development using Q-PCR (Figure 20C). Dlgap1, whose protein product is a core component of postsynaptic density (PSD), shows an over 20-fold increase in cRNA in P30 stage comparing with E18 stage, whilst the TTO only increased 5-fold. Myst4 also named Kat6b, associated with Ohdo syndrome and Genitopatellar syndrome,(Campeau et al., 2012), shows drastic increase in cRNA form but stay unchanged in TTO, while for Ezh2, both linear and circular form were down-regulated as neurons matured.

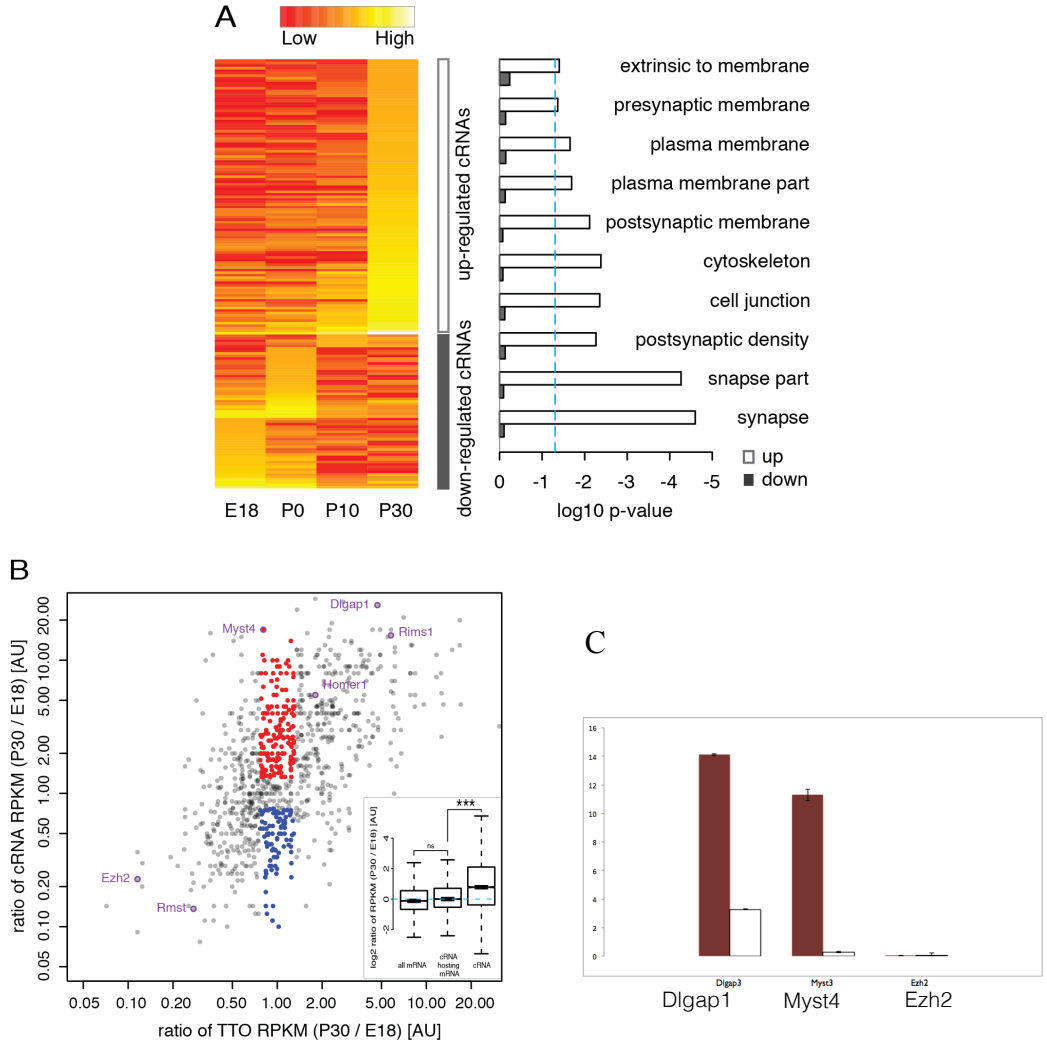

Figure 20. Expression of circular RNAs in brain during development. (A) Heatmap of cRNAs showed bipartite expression with the changing point at P10, a stage when synapses begins to form. Relative abundance across four developmental stages was encoded from blue (low) to red (high). The enriched GO terms were listed to the right. Hosting gene with cRNAs highly expressed in early stages were associated with regulation of transcription, whilst gene with cRNAs highly expressed in later stages were associated with synapse, vesicle and neuron projection. **(B)** Plot of both cRNAs (Y-axis) and the total transcriptional output of their gene loci (X-axis) between stage E18 andP30. Each dot represents one cRNA. **(C)** The expression change of Dlgap1, Myst4 and Ezh2 validated by qPCR. (red bars -cRNA transcript, white bars-linear transcripts of a same gene locus).

4.9 Expression change of circular RNAs after neuron stimulation

If cRNAs regulate synaptic function, their expression levels might be modulated by alterations in neuronal activity and plasticity. To test this hypothesis, we induced homeostatic synaptic plasticity in cultured hippocampal neurons by manipulating neuronal activity using bicuculline, an antagonist to the GABAa receptor. Addition of bicuculline results in enhanced excitatory neuronal activity and causes homeostatic scaling of synaptic responses (Krishek et al., 1996). Following exposure to bicuculline for 12 hrs, the cRNA expressed changed upon stimulation (Figure 21A). Many cRNAs change their expression independent of their hosting mRNAs as a result of bicuculine induced homeostatic plasticity, although as a group, the expression of cRNAs, correlate modestly with the total transcriptional output (TTO) of their gene loci (Figure 21B). A candidate circular RNA which stands out is Homer1, whose protein product is known as an immediate early gene which expression (short Homer1a isoform) is induced by neuronal activity and is considered to be a part of a mechanism of homeostatic plasticity that lowers the neuronal responsiveness when input activity is too high, while long form Homer1c plays a role in synaptic plasticity and the stabilization of synaptic changes during long-term potentiation (Shiraishi-Yamaguchi, 2007). Circular Homer1 showed an 8-fold increase upon bicuculine treatment while linear Homer1 increased about 2-fold. We validated sequencing results with qPCR for Homer1 and several other candidates. While the fold increase observed in sequencing was higher than the change observed by qPCR, the same trend remained. I addition, *in situ* validation of Homer shows the presence of circaHomer1 transcript (green puncta) within the cell body and dendritic arbor (Figure 21C).

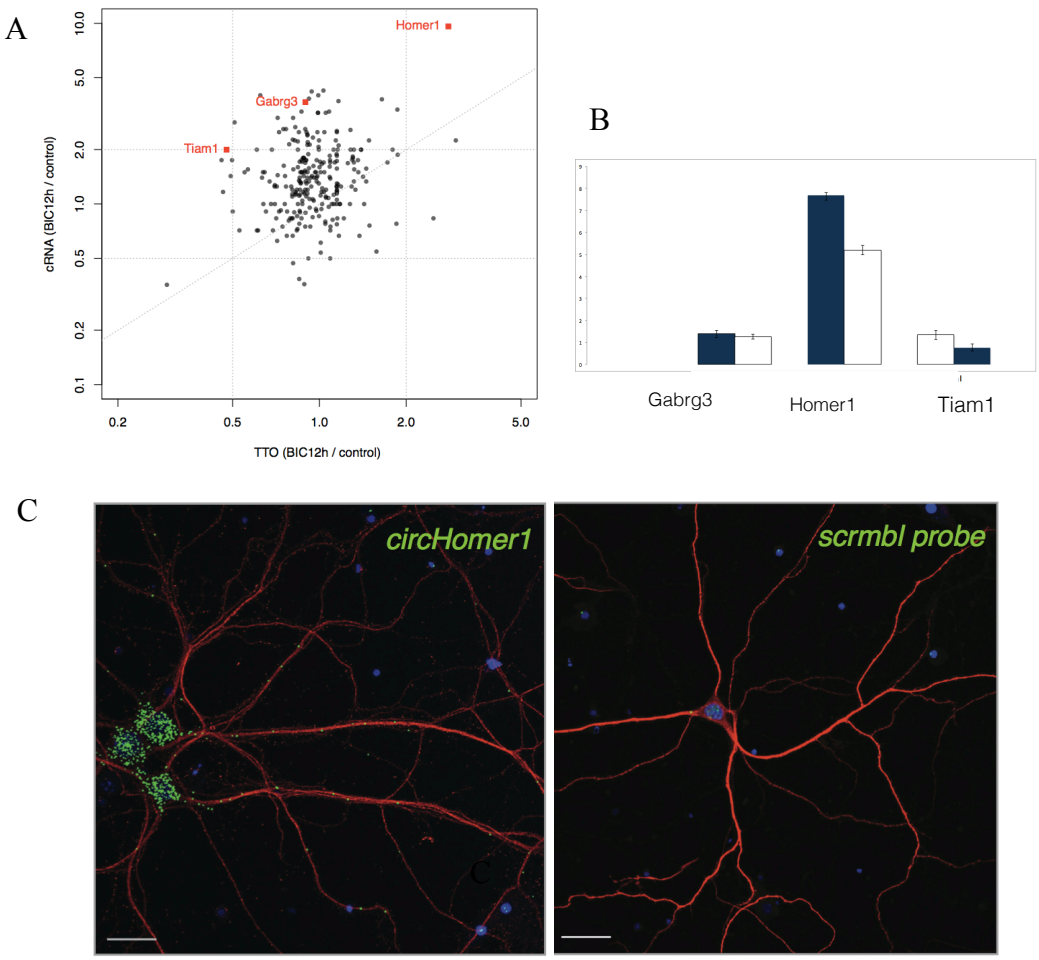

Figure 21. Expression change of circular RNAs after neuron stimulation. (A) Expression changes of cRNA (Y-axis) and TTO (X-axis) after 12hrs bicuculline treatment. Scatter plot illustrates the expression difference of of both cRNAs (Y-axis) and the total transcriptional output of their gene loci (X-axis) after 12hrs of bicuculline treatment of rat primary hippocampal neurons. Each dot represents one cRNA . As a group, the expression of cRNAs correlate with the total transcriptional output (TTO) of their gene loci (Figure 4B). Many cRNAs change their expression independent of their hosting mRNAs. (B) Q-PCR validated the expression change for three cRNA/mRNA pairs, (blue bars represent cRNA transcript, white bars represent linear transcripts of a same gene locus). (C) Fluorescent in situ hybridization (FISH) signal in cultured hippocampal neurons (DIV 21) showing the presence of circaHomer1 transcript (green particles) within the cell body and dendritic arbor. The neuron was immunostained with an antibody to MAP2 (green) to generate a mask that outlines the dendrites. Scale bar = 20 mm.

4.10 Circular RNAs co-purify components of an RNA transport granule

If circular RNAs are distally localized and enriched in synaptic fraction, in analogy to mRNAs, they should be actively transported to neuronal dendrites by molecular motors as a part of a large RNA transport granules. To search for the proteins involved in cRNA transport, we performed protein pull-down with in vitro transcript of 520 nt sequence of circular Homer1, as previously described (Huarte et al., 2010). In brief, biotin-labeled RNA was transcribed in vitro, immobilised on streptavidin magnetic beads and then incubated with mouse whole brain synaptosomes lysate. Complexes captured on the beads were subjected to stringent washes and finally eluted for SDS-PAGE. Pulldown samples using IVT transcribed Homer1,as well as negative control, i.e. antisense-Homer1 and beads, were subjected to protein identification using mass spectrometry. The protein abundance was estimated based on label free quantification (LFQ), where the relative intensities of the same peptide peaks in different runs reflect the relative abundance of proteins (Figure 22A). In total, we identified 403 proteins more than 5X enriched in Homer1 pulldown compared to a Homer1 antisense and beads only pulldown when setting a threshold value of MS intensity to (more than) 10^5. (Figure 22B).

To investigate the presence of RNA transport granule components among the enriched proteins in circular Homer1 pulldown in a systematic way, we extracted 42 proteins identified as a part of neuronal transport granule (a large detergent-resistant, RNase-sensitive granule, a binding partner of kinesin KIF5 in adult mouse brain (Kanai et al., 2004). Out of these 42 proteins from Kanai et al, we found 31 with 5-fold enrichment in Homer1 pulldown versus antisense negative control. Moreover, 8 out of 31 proteins were reported in an independent study of RNA transport granule in developing mouse brain (Elvira et al., 2006).

To validate the enrichment of proteins in Homer1 pulldown identified based on mass spectrometry data, we performed WB for two proteins, Fragile X mental retardation protein (FMRP), known regulator of protein synthesis at excitatory synapses and heterogeneous nuclear ribonucleoprotein (HnRNP-A2B1), ubiquitously expressed RNA-binding protein. Both proteins showed significant enrichment in Homer1 pulldown compared to a Homer1 antisense and beads only pulldowns.

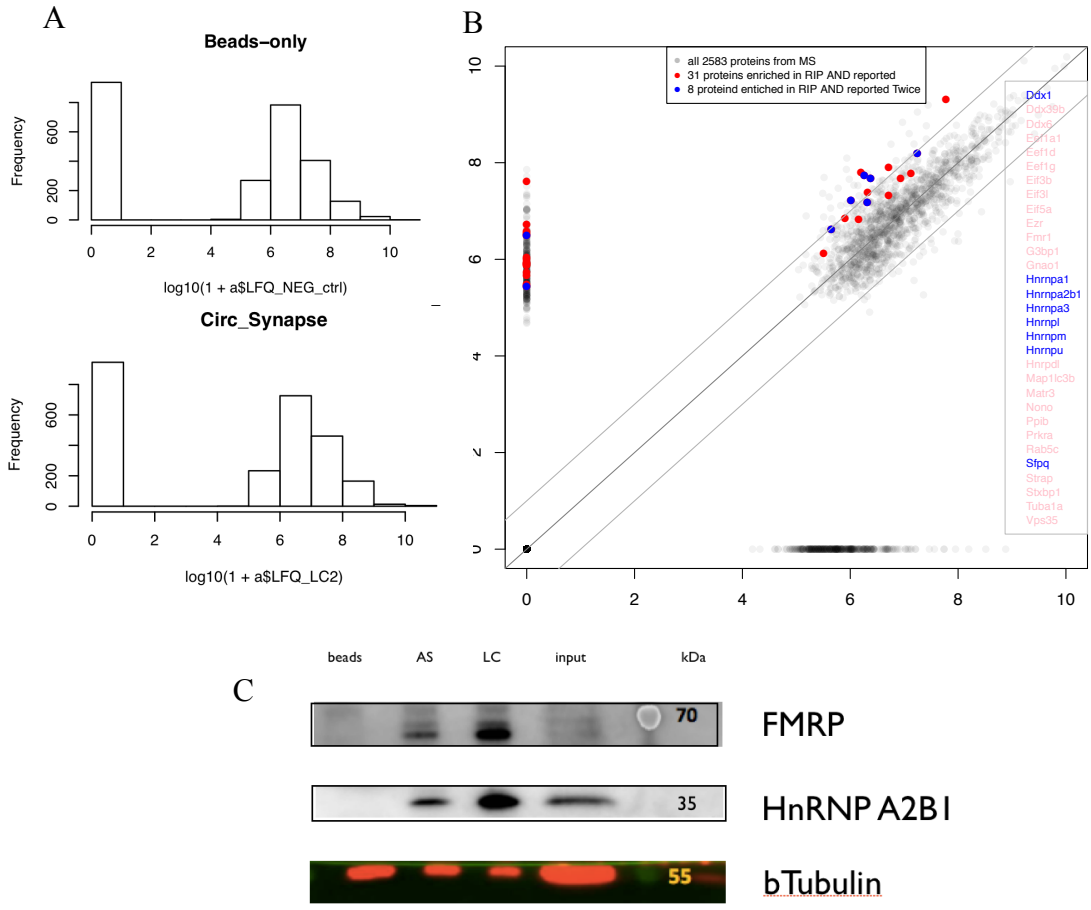

Figure 22. MS for circHomer1 RNA pulldown (A) The sum of LFQ are similar across the experiments, As equal amount of proteins are loaded for MS for all the sample analyzed. Entire protein lysate from RNA pull-down experiment from mouse whole brain synaptosomes was analyzed by liquid chromatography mass spectrometry (LC-MS). **(B)** Proteins were identified by searching the MS-generated data against the mouse International Protein Index protein sequence databases. Scatter plot depicts the difference in LFQ (Label Free Quantification) values of detected proteins as a proxy of protein abundance between Homer1 exon 2-5 (y-axis) and ‘‘no RNA’’ (beads only) (x-axis) RNA pull-down from. Proteins above the diagonal line are more than 5-fold enriched, previously detected as part of RNA transport granules. Literature examples are marked in blue&red (Kanai & Elvira). **(C)**Two candidates identified in MS were confirmed by western blot: hnRNPA2/B1 and FMRP. After byotinilated RNA pull-down, the eluate was resolved on SDS-PAGE for western blotting. ‘‘no RNA’’ (beads only) sample served as negative controls. Bands corresponding to hnRNPA2/B1 and FMRP were observed in Homer1 exon 2-5 and and AS-Homer1 but were clearly enriched in Homer1 exon 2-5. Beta- tubulin served as a loading control.

5. DISCUSSION

In recent years, the understanding of signalling in dendritic and axonal compartments has been revolutionised with the recognition of a variety of RNA molecules and their multiple functions in regulation of protein translation and other cellular functions.

In this study we demonstrated that synaptosomes are reliable source for studying gene expression in synaptic region. We further expanded the number of synaptic mRNAs and discovered a remarkable synaptic localization pattern for a subset of TF transcripts. Next, we demonstrated circular RNAs are most abundant in brain, enriched in synaptic fraction and transported as a part of a RNA transport granule. Furthermore, we showed that levels of cRNA changed during neuron development, and are modulated by alternations in neuronal activity and plasticity. .

5.1 Genome-wide expression profiling of synaptosomes

The main obstacle for studies of local population of molecules in the synaptic region is the technical difficulty in obtaining pure and sufficient quantities of axons and dendrites. To date, experiments dealing with the local translation in neuron are performed either on microfluidically isolated dendrites and axons, from microdissected neuropil or on synaptosomes. Synaptosomes isolation protocols have been constantly developed, for more than 50 years, since the initial nerve terminal preparations introduced by Gray and Whittaker in 1962. The optimization was in the direction of increasing the fraction of synaptosome within the sample, improving the synaptosome viability for downstream applications and reducing the time needed for isolation. That is how Percoll was introduced because of two major advantages: (i) it

has low viscosity, allowing more rapid sedimentation and use of lower centrifugal forces than that required for sucrose and Ficoll and (ii) it can be prepared in an isotonic solution (such as isotonic sucrose) to maintain osmolarity. Synaptosomes, a resealed membraneous vesicles formed from pinched off nerve terminal, are a convenient system for studies in sub-neuronal compartments because of the perservance of molecular machinery used in neuronal signaling as well as capability of uptake, storage, and release of neurotransmitters. Without further purification synaptosomes are compatible with a variety of molecular biology techniques, including immunoprecipitation, western blotting, monitoring *de novo* protein synthesis, electron microscopy, and a variety of enzyme activity assays. However, the use of RNA based techniques with synaptosomes was delayed due to the low quality and low yields of RNA obtained through the standard purification protocols.

Here we demonstrated that poor quality of RNA obtained from Percoll gradient procedure is a result of PVP coating of Percoll reagent, which is incompatible with phenol-chlorophorm and silica membrane-based methods for RNA isolation. We show that this can be successfully solved by using Percoll Plus reagent which is coated with silan. With Percoll Plus gradient incorporated into the synaptosome isolation procedure, we obtained RNA of high quality, a prerequisite for reproducible transcriptome sequencing. In future, it will be interesting to apply our protocol together with other RNA profiling approaches, as for example with ribosome profiling that uses deep sequencing to monitor in vivo translation to estimate the efficiency and identity of newly synthesized protein to gain new insights into synaptic local translation. Further, synaptosomes have been prepared from more than ten different rodent brain regions, including cerebrum (Wittzman et al., 2005), striatum (Rapier et al., 1990), cerebellum (Terrian et al, 1988) hippocampus (Thorne et al, 1991), and the neurohypophysis (Nordman et al, 1988), therefore our protocol could be used to

characterize the distribution of coding and non coding transcripts in the synaptic part of the cell from different regions of mammalian brain.

5.2 The landscape of synaptic mRNAs

Localized mRNAs have been observed in numerous cell types from yeast to human, but only recently with the development of methods for genome wide expression profiling it is possible to address the prevalence of RNA localization. In neurons the extent of RNA localization has impact on local translation and subsequent forming of distinct postsynaptic domains. Here, using next generation sequencing of hippocampal synaptosomes, we confirmed and broaden the findings from Cajigas et al. 2012, where they identified a surprisingly large number of previously undetected neuropil mRNAs, which led to the estimation that greater than one-half of the hippocampal CA1 neuron transcriptome can be detected in the axons and dendrites. Based on the current reference database (Ensembl, *Mus musculus* transcriptome), we estimate that the number of unique transcripts associated with the various cells and compartments (axons, dendrites, glia, and interneurons) enriched in mouse hippocampal synaptosome preparation is about 11, 303 mRNAs, 2, 924 more than the entire hippocampal neuropil set from Cajigas et al., 2012. More conservative estimate, based on the proposed criteria from Cajigas et al., 2012 after subtraction of genes that are overrepresented in other cell types (glia, interneurons) or compartments (mitochondria and nucleus), we arrive at a dendritic-axonal data set of 4,863 mRNAs, 2,356 more than hippocampal neuropil set from Cajigas et al., 2012. In summary, our data sets confirm previous findings and suggest the local transcriptome might comprise of an even higher number of transcripts. The increased number of transcripts

detected in our study results from a higher sensitivity of the next generation sequencing technology used.

Further, the comparison of the mRNA abundance between mouse hippocampal synaptosome and the whole hippocampus showed that synaptic regions harbours a population of RNAs that are probably actively transported to the distal processes, if assuming random diffusion would not result in the enrichment of a subset of transcripts. In addition, GO analysis showed the transcripts derived from the genes with nuclear function are by large depleted, indicating the synaptosomes are free from cell body contamination. In future, it will be interesting to further investigate transcript abundance differences between two complementary methods for capturing neuronal local transcriptome, since neuropil might represent the localization highway while synaptosomes are more specialized subcellular structures, more closely related to synapse.

5.3 TF at the synapse

Synaptic plasticity-regulated gene expression is considered a key event in the long-lasting changes of neuronal function, essential for learning and memory and several mechanisms have been proposed to explain long distance communication between synapses and the nucleus. One model suggests that synaptic activity triggers the translocation of certain TFs and TF regulators localized at postsynaptic sites to the nucleus, although transcription factors as critical regulators of gene expression are primarily thought to be restricted to the nucleus and surrounding cell soma. Here, we show by large, depletion of majority of known TF from synaptosomes. However, we also found a subset of more than 45 moderately to highly expressed TF that are at

least two fold enriched in mouse hippocampal synaptosomes. We independently validated the presence for several of them by ISH in primary hippocampal neurons. Since it has been proposed that local translation and translocation of TF from postsynaptic sites to the nucleus is part of a synapse-to-nucleus signalling cascade in key neuronal processes like circadian rhythms, long- term memory and neuronal survival (Diesseroth, 2003) and in recent years a number of potential synapto-nuclear protein messengers such as Abi-1, AIDA-1D, CREB2, Jacob, NfκB, and the Wnt receptors have been identified (Jordan and Kreutz, 2009; Budnik and Salinas, 2011), in future, it will be interesting to investigate the potential role of those factors in synapse-to-nucleus signaling. Alternative model to explain the prevalence of mRNAs for nuclear proteins residing at the synapse is that some of these transcripts encoded proteins may have novel non-nuclear functions, as for example Elk-1 with both, nuclear function, and non-nuclear one related to mitochondria (Barrett et al., 2006).

5.4 Systematic profiling of circular RNA across different mouse tissues reveals ist enrichment in the brain and enrichment in neuronal distal compartments

Recently, the number of known circRNA transcripts in mammalian cells has been greatly expanded. Here we focused primarily on the genome- wide circular RNA characterization in the brain and its subcellular localization pattern. We applied a non-candidate based approach by identifing RNA-seq reads consisting of apparent back splice sequences from rRNA depleted samples across different mouse tissues. After choosing the reads that could not be mapped directly to the genome, we mapped their two end parts separately and thereby identified the location of a potential back splice to a single-nucleotide resolution. We selected only apparent back splice sequences that are flanked by GT/AG splice sites in the genomic context, without relying on the

known gene annotation, therefore the method we used here is more sensitive than candidate based approach. We found that reads mapping to the circular junction reads comprise about 0.1 % reads form all rRNA depleted total RNA which is similar to a recent estimate obtained from human fibroblasts (Jeck et al., 2013).

Further, we characterized the tissue-specific circular RNA profile in brain with regard to the expression of cRNAs in liver, lung, testis and heart. The percentage of circular junction reads from all the reads mapped on Ensembl protein coding genes were highest in brain and testis. Much lower expression of cRNA was observed in other tissues. This is not surprising knowing that muscle and liver have the least complex transcriptomes expressing predominantly ubiquitous genes with a large fraction of the transcripts coming from a few highly expressed genes, whereas brain, kidney and testis express more complex transcriptomes with the majority of genes expressed and relatively small contributions from highly expressed genes. Yet, neuronal function is highly dependent on spatially precise signaling that occurs in restricted subcellular domains. This is accomplished by the localization of both protein-coding and noncoding RNA in neuronal processes and the subsequent regulated local translation of mRNA into protein. Here we show for the first time that substanital portion of circular RNAs detected in the brain are highly abundant and enirched in synaptic region. We examined dynamics of the two fundamental neuronal processes, synaptic development and plasticity. We found that exonic cRNA changed abundance upon neuranal stimultion or during development. For some, such change in cRNA expression is independent of the host linear gene. The changes observed by sequencing could be independently validated with qPCR for circular and linear transcripts induced at 12 hours following neuronal activity and in the hippocampus of developmental stages of embyonic day 18 (E18) and postnatal day 30 (P30) .

5.5 Circular RNAs are components of mRNA transport granules

The previously unappreciated abundance and diversity of circular RNAs at the synapse raises an important question: What is the molecular mechanism underlying circular RNA transport? Here we have shown that circular RNAs could co-purify components of neuronal RNA transport granule, a non-membranous vesicles, based on reversible aggregation of the RBPs and mRNAs destined for dendritic localization These granules are dynamic and are able to interact with each other and with active polysomes providing cell with the mechanisms to adjust translation to the environmental changes. Therefore, it will be interesting to further investigate the dynamics and localization of circular RNAs and RBPs as well as miRNAs within different types of RNA granules.

CONCLUSION

In conclusion, in this study, using an unbiased approach, we have characterized distally localized (1) coding and (2) non-coding neuronal transcriptome. Taken together our data serves an important resources for further functional study of RNA localization and local regulation in neuron.

REFERENCES

Aakalu, G., Smith, W. B., Nguyen, N., Jiang, C., & Schuman, E. M. (2001). Dynamic Visualization of Local Protein Synthesis in Hippocampal Neurons. *Neuron*, *30*(2), 489–502. doi:10.1016/S0896-6273(01)00295-1

Aigner, L., & Caroni, P. (1993). Depletion of 43-kD growth-associated protein in primary sensory neurons leads to diminished formation and spreading of growth cones. *The Journal of Cell Biology*, *123*(2), 417–429. doi:10.1083/jcb.123.2.417

Ameres, S. L., & Zamore, P. D. (2013). Diversifying microRNA sequence and function. *Nature Reviews Molecular Cell Biology*, *14*(8), 475–488. doi:10.1038/nrm3611

An, J. J., Gharami, K., Liao, G.-Y., Woo, N. H., Lau, A. G., Vanevski, F., et al. (2008). Distinct Role of Long 3′ UTR BDNF mRNA in Spine Morphology and Synaptic Plasticity in Hippocampal Neurons. *Cell*, *134*(1), 175–187. doi:10.1016/j.cell.2008.05.045

Anderson, P., & Kedersha, N. (2009). RNA granules: post-transcriptional and epigenetic modulators of gene expression. *Nature Reviews Molecular Cell Biology*, *10*(6), 430–436. doi:10.1038/nrm2694

Andreassi, C., Zimmermann, C., Mitter, R., Fusco, S., Devita, S., Saiardi, A., & Riccio, A. (2010). An NGF-responsive element targets myo-inositol monophosphatase-1 mRNA to sympathetic neuron axons (vol 13, pg 291, 2010). *Nat Neurosci , 13 (8) 1033 - 1033. (2010)*, *13*(8), 1033–1033. doi:10.1038/nn0810-1033a

Arimura, N., & Kaibuchi, K. (2007). Neuronal polarity: from extracellular signals to intracellular mechanisms. *Nature Reviews Neuroscience*, *8*(3), 194–205. doi:10.1038/nrn2056

Barrett, L. E., Sul, J.-Y., Takano, H., Van Bockstaele, E. J., Haydon, P. G., & Eberwine, J. H. (2006). Region-directed phototransfection reveals the functional significance of a dendritically synthesized transcription factor. *Nature Methods*, *3*(6), 455–460. doi:10.1038/nmeth885

Bhakar, A. L., Dölen, G., & Bear, M. F. (2012). The Pathophysiology of Fragile X (and What It Teaches Us about Synapses). *Annual Review of Neuroscience*, *35*(1), 417–443. doi:10.1146/annurev-neuro-060909-153138

Bliss, T. V., & Gardner-Medwin, A. R. (1973). Long-lasting potentiation of synaptic transmission in the dentate area of the unanaestetized rabbit following stimulation of the perforant path. *The Journal of Physiology*, *232*(2), 357–374.

Budnik, V., & Salinas, P. C. (2011). Wnt signaling during synaptic development and plasticity. *Current Opinion in Neurobiology*.

Bunge, M. B. (1973). FINE STRUCTURE OF NERVE FIBERS AND GROWTH CONES OF ISOLATED SYMPATHETIC NEURONS IN CULTURE. *The Journal of Cell Biology*, *56*(3), 713–735. doi:10.1083/jcb.56.3.713

Burgin, K. E., Waxham, M. N., Rickling, S., Westgate, S. A., Mobley, W. C., & Kelly, P. T. (1990). In situ hybridization histochemistry of Ca2+/calmodulin-dependent protein kinase in developing rat brain. *The Journal of Neuroscience*, *10*(6), 1788–1798.

Buxbaum, A. R., Bin, W., & Singer, R. H. (n.d.). Single β-Actin mRNA Detection in Neurons Reveals a Mechanism for Regulating Its Translatability
.

Cahoy, J. D., Emery, B., Kaushal, A., Foo, L. C., Zamanian, J. L., Christopherson, K. S., et al. (2008). A transcriptome database for astrocytes, neurons, and oligodendrocytes: a new resource for understanding brain development and function. *The Journal of Neuroscience*, *28*(1), 264–278. doi:10.1523/JNEUROSCI.4178-07.2008

Cajigas, I. J., Tushev, G., Will, T. J., tom Dieck, S., Fuerst, N., & Schuman, E. M. (2012). The Local Transcriptome in the Synaptic Neuropil Revealed by Deep Sequencing and High-Resolution Imaging. *Neuron*, *74*(3), 453–466. doi:10.1016/j.neuron.2012.02.036

Cajigas, I. J., Will, T., & Schuman, E. M. (2010). Protein homeostasis and synaptic plasticity. *The EMBO Journal*, *29*(16), 2746–2752. doi:10.1038/emboj.2010.173

Campbell, D. S., & Holt, C. E. (2001). Chemotropic Responses of Retinal Growth Cones Mediated by Rapid Local Protein Synthesis and Degradation. *Neuron*, *32*(6), 1013–1026. doi:10.1016/S0896-6273(01)00551-7

Campeau, P. M., Lu, J. T., Dawson, B. C., Fokkema, I. F. A. C., Robertson, S. P., Gibbs, R. A., & Lee, B. H. (2012). The KAT6B−related disorders genitopatellar syndrome and Ohdo/SBBYS syndrome have distinct clinical

features reflecting distinct molecular mechanisms. *Human Mutation*, *33*(11), 1520–1525. doi:10.1002/humu.22141

Castello, A., Fischer, B., Eichelbaum, K., Horos, R., Beckmann, B. M., Strein, C., et al. (2012). Insights into RNA biology from an atlas of mammalian mRNA-binding proteins. *Cell*, *149*(6), 1393–1406. doi:10.1016/j.cell.2012.04.031

Chao, W. (2007). formin(Fmn)Gene:Abundant CircularRNA TranscriptsandGene-Targeted Deletion Analysis, 1–15.

Chen, C., & Sarnow, P. (1995). Initiation of protein synthesis by the eukaryotic translational apparatus on circular RNAs. *Science-New York Then Washington*.

Citri, A., & Malenka, R. C. (2008). Synaptic plasticity: multiple forms, functions, and mechanisms. *Neuropsychopharmacology : Official Publication of the American College of Neuropsychopharmacology*, *33*(1), 18–41. doi:10.1038/sj.npp.1301559

Cocquerelle, C., Mascrez, B., Hétuin, D., & Bailleul, B. (1993). Mis-splicing yields circular RNA molecules. *FASEB Journal : Official Publication of the Federation of American Societies for Experimental Biology*, *7*(1), 155–160.

Cocquet, J., Chong, A., Zhang, G., & Veitia, R. A. (2006). Reverse transcriptase template switching and false alternative transcripts. *Genomics*, *88*(1), 127–131. doi:10.1016/j.ygeno.2005.12.013

Consortium, T. E. P. (2012). An integrated encyclopedia of DNA elements in the human genome. *Nature*, *489*(7414), 57–74. doi:10.1038/nature11247

Costa-Mattioli, M., Gobert, D., Harding, H., Herdy, B., Azzi, M., Bruno, M., et al. (2005). Translational control of hippocampal synaptic plasticity and memory by the eIF2α kinase GCN2. *Nature Cell Biology*, *436*(7054), 1166–1173. doi:10.1038/nature03897

Coulon, A., Chow, C. C., Singer, R. H., Larson, D. R., coulon. (2013). Eukaryotic transcriptional dynamics: from single molecules to cell populations. *Nature Reviews Genetics*, *14*(8), 572–584. doi:10.1038/nrg3484

Crick, F. (1970). Central dogma of molecular biology. *Nature*, *227*(5258), 561–563.

Daneman, R., Zhou, L., Kebede, A. A., & Barres, B. A. (2010). Pericytes are required for blood–brain barrier integrity during embryogenesis. *Nature*, *468*(7323), 562–566. doi:10.1038/nature09513

Darnell, J. C., Van Driesche, S. J., Zhang, C., Hung, K. Y. S., Mele, A., Fraser, C. E., et al. (2011). FMRP Stalls Ribosomal Translocation on mRNAs Linked to Synaptic Function and Autism. *Cell*, *146*(2), 247–261. doi:10.1016/j.cell.2011.06.013

De Robertis, E., De Iraldi, A. P., & Rodriguez, G. (1961). On the isolation of nerve endings and synaptic vesicles. *The Journal of …*.

Deglincerti, A., & Jaffrey, S. R. (2012). Insights into the roles of local translation from the axonal transcriptome. *Open Biology*, *2*(6), 120079–120079. doi:10.1098/rsob.120079

Deisseroth, K., Mermelstein, P. G., Xia, H., & Tsien, R. W. (2003). Signaling from synapse to nucleus: the logic behind the mechanisms. *Current Opinion in Neurobiology*, *13*(3), 354–365.

Di Giammartino, D. C., Nishida, K., & Manley, J. L. (2011). Mechanisms and consequences of alternative polyadenylation. *Molecular Cell*, *43*(6), 853–866. doi:10.1016/j.molcel.2011.08.017

Donnelly, C. J., Fainzilber, M., & Twiss, J. L. (2010). Subcellular communication through RNA transport and localized protein synthesis. *Traffic (Copenhagen, Denmark)*, *11*(12), 1498–1505. doi:10.1111/j.1600-0854.2010.01118.x

Dubin, R. A., Kazmi, M. A., & Ostrer, H. (1995). Inverted repeats are necessary for circularization of the mouse testis Sry transcript. *Gene*, *167*(1-2), 245–248. doi:10.1016/0378-1119(95)00639-7

Dunkley, P. R., Jarvie, P. E., & Robinson, P. J. (2008). A rapid Percoll gradient procedure for preparation of synaptosomes. *Nature Protocols*, *3*(11), 1718–1728. doi:10.1038/nprot.2008.171

Ebert, M. S., & Sharp, P. A. (2010). MicroRNA sponges: progress and possibilities. *Rna*, *16*(11), 2043–2050. doi:10.1261/rna.2414110

Edbauer, D., Neilson, J. R., Foster, K. A., Wang, C.-F., Seeburg, D. P., Batterton, M. N., et al. (2010). Regulation of Synaptic Structure and Function by FMRP-Associated MicroRNAs miR-125b and miR-132. *Neuron*, *65*(3), 373–384. doi:10.1016/j.neuron.2010.01.005

Elvira, G., Wasiak, S., Blandford, V., Tong, X.-K., Serrano, A., Fan, X., et al. (2006). Characterization of an RNA granule from developing brain. *Molecular & Cellular Proteomics : MCP*, *5*(4), 635–651. doi:10.1074/mcp.M500255-MCP200

Fiore, R., Khudayberdiev, S., Saba, R., & Schratt, G. (2011). MicroRNA function in the nervous system. *Progress in Molecular Biology and Translational Science*, *102*, 47–100. doi:10.1016/B978-0-12-415795-8.00004-0

Flexner, J. B., Flexner, L. B., & Stellar, E. (1963). Memory in Mice as Affected by Intracerebral Puromycin. *Science (New York, N.Y.)*, *141*(3575), 57–59. doi: 10.1126/science.141.3575.57

Garner, C. C., Tucker, R. P., & Matus, A. (1988). Selective localization of messenger RNA for cytoskeletal protein MAP2 in dendrites. *Nature*, *336*(6200), 674–677. doi:10.1038/336674a0

Gu, W., Pan, F., Zhang, H., Bassell, G. J., & Singer, R. H. (2002). A predominantly nuclear protein affecting cytoplasmic localization of beta-actin mRNA in fibroblasts and neurons. *The Journal of Cell Biology*, *156*(1), 41–51. doi: 10.1083/jcb.200105133

Gualandi, F., Trabanelli, C., Rimessi, P., Calzolari, E., Toffolatti, L., Patarnello, T., et al. (2003). Multiple exon skipping and RNA circularisation contribute to the severe phenotypic expression of exon 5 dystrophin deletion. *Journal of Medical Genetics*, *40*(8), e100–e100. doi:10.1136/jmg.40.8.e100

Guo, H., Ingolia, N. T., Weissman, J. S., & Bartel, D. P. (2010). Mammalian microRNAs predominantly act to decrease target mRNA levels. *Nature*, *466*(7308), 835–840. doi:10.1038/nature09267

Hansen, T. B., Jensen, T. I., Clausen, B. H., Bramsen, J. B., Finsen, B., Damgaard, C. K., & Kjems, J. (2013). Natural RNA circles function as efficient microRNA sponges. *Nature*, *495*(7441), 384–388. doi:10.1038/nature11993

Harris, W. A., Holt, C. E., & Bonhoeffer, F. (1987). Retinal axons with and without their somata, growing to and arborizing in the tectum of Xenopus embryos: a time-lapse video study of single fibres in vivo. *Development*, *101*(1), 123–133.

Hawkins, R. D., Hon, G. C., & Ren, B. (2010). Next-generation genomics: an integrative approach. *Nature Reviews Genetics*.

Hentze, M. W., & Preiss, T. (2013). Circular RNAs: splicing's enigma variations. *The EMBO Journal*, *32*(7), 923–925. doi:10.1038/emboj.2013.53

Holt, C. E., & Schuman, E. M. (2013). The Central Dogma Decentralized: New Perspectives on RNA Function and Local Translation in Neurons. *Neuron*, *80*(3), 648–657. doi:10.1016/j.neuron.2013.10.036

Hsu, M. T., & Coca-Prados, M. (1979). Electron microscopic evidence for the circular form of RNA in the cytoplasm of eukaryotic cells. *Nature*, *280*(5720), 339–340.

Huang, Y.-S., Carson, J. H., Barbarese, E., & Richter, J. D. (2003). Facilitation of dendritic mRNA transport by CPEB. *Genes & Development*, *17*(5), 638–653. doi:10.1101/gad.1053003

Huarte, M., Guttman, M., Feldser, D., Garber, M., Koziol, M. J., Kenzelmann-Broz, D., et al. (2010). A Large Intergenic Noncoding RNA Induced by p53 Mediates Global Gene Repression in the p53 Response. *Cell*, *142*(3), 409–419. doi:10.1016/j.cell.2010.06.040

Hüttelmaier, S., Zenklusen, D., Lederer, M., Dictenberg, J., Lorenz, M., Meng, X., et al. (2005). Spatial regulation of beta-actin translation by Src-dependent phosphorylation of ZBP1. *Nature*, *438*(7067), 512–515. doi:10.1038/nature04115

Jambhekar, A., & DeRisi, J. L. (2007). Cis-acting determinants of asymmetric, cytoplasmic RNA transport. *Rna*, *13*(5), 625–642. doi:10.1261/rna.262607

Jeck, W. R., & Sharpless, N. E. (2014). Detecting and characterizing circular RNAs. *Nature Biotechnology*, *32*(5), 453–461. doi:10.1038/nbt.2890

Jeck, W. R., Sorrentino, J. A., Wang, K., Slevin, M. K., Burd, C. E., Liu, J., et al. (2013). Circular RNAs are abundant, conserved, and associated with ALU repeats. *Rna*, *19*(2), 141–157. doi:10.1261/rna.035667.112

Jin, P., Alisch, R. S., & Warren, S. T. (2004). RNA and microRNAs in fragile X mental retardation. *Nature Cell Biology*, *6*(11), 1048–1053. doi:10.1038/ncb1104-1048

Jordan, B. A., & Kreutz, M. R. (2009). Nucleocytoplasmic protein shuttling: the direct route in synapse-to-nucleus signaling. *Trends in Neurosciences*.

Kamme, F., Salunga, R., Yu, J., Tran, D.-T., Zhu, J., Luo, L., et al. (2003). Single-cell microarray analysis in hippocampus CA1: demonstration and validation of cellular heterogeneity. *The Journal of Neuroscience*, *23*(9), 3607–3615.

Kanai, Y., Dohmae, N., & Hirokawa, N. (2004). Kinesin Transports RNA. *Neuron*, *43*(4), 513–525. doi:10.1016/j.neuron.2004.07.022

Kandel, E. R. (2001). The molecular biology of memory storage: a dialogue between genes and synapses. *Science (New York, N.Y.)*, *294*(5544), 1030–1038. doi: 10.1126/science.1067020

Kang, H., & Schuman, E. M. (1996). A requirement for local protein synthesis in neurotrophin-induced hippocampal synaptic plasticity. *Science (New York, N.Y.)*, *273*(5280), 1402–1406.

Keene, J. D., & Lager, P. J. (2005). Post-transcriptional operons and regulons co-ordinating gene expression. *Chromosome Research*, *13*(3), 327–337. doi: 10.1007/s10577-005-0848-1

Kelleher, R. J., III, Govindarajan, A., & Tonegawa, S. (2004). Translational Regulatory Mechanisms in Persistent Forms of Synaptic Plasticity. *Neuron*, *44*(1), 59–73. doi:10.1016/j.neuron.2004.09.013

Kellis, M., Wold, B., Snyder, M. P., Bernstein, B. E., Kundaje, A., Marinov, G. K., et al. (2014). Defining functional DNA elements in the human genome. *Pnas*, *111*(17), 6131–6138. doi:10.1073/pnas.1318948111

Kiebler, M. A., & Bassell, G. J. (2006). Neuronal RNA Granules: Movers and Makers. *Neuron*, *51*(6), 685–690. doi:10.1016/j.neuron.2006.08.021

Klausberger, T., & Somogyi, P. (2008). Neuronal diversity and temporal dynamics: the unity of hippocampal circuit operations. *Science (New York, N.Y.)*, *321*(5885), 53–57. doi:10.1126/science.1149381

Knowles, R. B., Sabry, J. H., Martone, M. E., Deerinck, T. J., Ellisman, M. H., Bassell, G. J., & Kosik, K. S. (1996). Translocation of RNA granules in living neurons. *The Journal of Neuroscience*, *16*(24), 7812–7820.

Kornblihtt, A. R., Schor, I. E., oacute, M. A., Dujardin, G., Petrillo, E., & oz, M. J. M. N. (2013). Alternative splicing: a pivotal step between eukaryotic transcription and translation. *Nature Reviews Molecular Cell Biology*, *14*(3), 153–165. doi: 10.1038/nrm3525

Krichevsky, A. M., & Kosik, K. S. (2001). Neuronal RNA GranulesA Link between RNA Localization and Stimulation-Dependent Translation. *Neuron*, *32*(4), 683–696. doi:10.1016/S0896-6273(01)00508-6

Kye, M.-J., Liu, T., Levy, S. F., Xu, N. L., Groves, B. B., Bonneau, R., et al. (2007). Somatodendritic microRNAs identified by laser capture and multiplex RT-PCR. *Rna*, *13*(8), 1224–1234. doi:10.1261/rna.480407

Lee, H. Y., Ge, W.-P., Huang, W., He, Y., Wang, G. X., Rowson-Baldwin, A., et al. (2011). Bidirectional Regulation of Dendritic Voltage-Gated Potassium Channels by the Fragile X Mental Retardation Protein. *Neuron*, *72*(4), 630–642. doi:10.1016/j.neuron.2011.09.033

Lécuyer, E., Yoshida, H., Parthasarathy, N., Alm, C., Babak, T., Cerovina, T., et al. (2007). Global Analysis of mRNA Localization Reveals a Prominent Role in Organizing Cellular Architecture and Function. *Cell*, *131*(1), 174–187. doi:10.1016/j.cell.2007.08.003

Martin, K. C., & Ephrussi, A. (2009). mRNA localization: gene expression in the spatial dimension. *Cell*, *136*(4), 719–730. doi:10.1016/j.cell.2009.01.044

Matamales, M. (2012). Neuronal activity-regulated gene transcription: how are distant synaptic signals conveyed to the nucleus? *F1000Research*, *1*, 69. doi:10.12688/f1000research.1-69.v1

Mayford, M., Baranes, D., Podsypanina, K., & Kandel, E. R. (1996). The 3'-untranslated region of CaMKII alpha is a cis-acting signal for the localization and translation of mRNA in dendrites. *Proceedings of the National Academy of Sciences of the United States of America*, *93*(23), 13250–13255.

Mellman, I., & Nelson, W. J. (2008). Coordinated protein sorting, targeting and distribution in polarized cells. *Nature Reviews Molecular Cell Biology*, *9*(11), 833–845. doi:10.1038/nrm2525

Memczak, S., Jens, M., Elefsinioti, A., Torti, F., Krueger, J., Rybak, A., et al. (2013). Circular RNAs are a large class of animal RNAs with regulatory potency. *Nature*, 1–10. doi:10.1038/nature11928

Mercer, T. R., Gerhardt, D. J., Dinger, M. E., Crawford, J., Trapnell, C., Jeddeloh, J. A., et al. (2012). Targeted RNA sequencing reveals the deep complexity of the human transcriptome. *Nature Biotechnology*, *30*(1), 99–104. doi:10.1038/nbt.2024

Miller, S., Yasuda, M., Coats, J. K., Jones, Y., Martone, M. E., & Mayford, M. (2002). Disruption of Dendritic Translation of CaMKIIα Impairs Stabilization of Synaptic Plasticity and Memory Consolidation. *Neuron*, *36*(3), 507–519. doi:10.1016/S0896-6273(02)00978-9

Moore, M. J. (2005). From birth to death: the complex lives of eukaryotic mRNAs. *Science (New York, N.Y.)*, *309*(5740), 1514–1518. doi:10.1126/science.1111443

Muddashetty, R. S., Nalavadi, V. C., Gross, C., Yao, X., Xing, L., Laur, O., et al. (2011). Reversible Inhibition of PSD-95 mRNA Translation by miR-125a, FMRP Phosphorylation, and mGluR Signaling. *Molecular Cell*, *42*(5), 673–688. doi:10.1016/j.molcel.2011.05.006

Narayanan, U., Nalavadi, V., Nakamoto, M., Pallas, D. C., Ceman, S., Bassell, G. J., & Warren, S. T. (2007). Fragile X mental retardation protein deficiency leads to excessive mGluR5-dependent internalization of AMPA receptors. *Proceedings of the National Academy of Sciences of the United States of America*, *104*(39), 15537–15542. doi:10.1073/pnas.0707484104

Okaty, B. W., Sugino, K., & Nelson, S. B. (2011). A quantitative comparison of cell-type-specific microarray gene expression profiling methods in the mouse brain. *PLoS ONE*, *6*(1), e16493. doi:10.1371/journal.pone.0016493

Pal, S., Gupta, R., Kim, H., Wickramasinghe, P., Baubet, V., Showe, L. C., et al. (2011). Alternative transcription exceeds alternative splicing in generating the transcriptome diversity of cerebellar development. *Genome Research*, *21*(8), 1260–1272. doi:10.1101/gr.120535.111

Park, H. Y., Lim, H., Yoon, Y. J., Follenzi, A., Nwokafor, C., Lopez-Jones, M., et al. (2014). Visualization of dynamics of single endogenous mRNA labeled in live mouse. *Science (New York, N.Y.)*, *343*(6169), 422–424. doi:10.1126/science.1239200

Patel, V. L., Mitra, S., Harris, R., Buxbaum, A. R., Lionnet, T., Brenowitz, M., et al. (2012). Spatial arrangement of an RNA zipcode identifies mRNAs under post-transcriptional control. *Genes & Development*, *26*(1), 43–53. doi:10.1101/gad.177428.111

Pichardo-Casas, I., Goff, L. A., Swerdel, M. R., Athie, A., Davila, J., Ramos-Brossier, M., et al. (2012). Expression profiling of synaptic microRNAs from the adult rat brain identifies regional differences and seizure-induced dynamic modulation. *Brain Research*, *1436*, 20–33. doi:10.1016/j.brainres.2011.12.001

Poon, M. M., Choi, S.-H., Jamieson, C. A. M., Geschwind, D. H., & Martin, K. C. (2006). Identification of process-localized mRNAs from cultured rodent hippocampal neurons. *The Journal of Neuroscience*, *26*(51), 13390–13399. doi:10.1523/JNEUROSCI.3432-06.2006

Quattrone, A., Dahm, R., & Macchi, P. (2012). Subcellular RNA Localization and Translational Control. *RNA Binding Proteins*.

Qureshi, I. A., & Mehler, M. F. (2012). Emerging roles of non-coding RNAs in brain evolution, development, plasticity and disease. *Nature Reviews Neuroscience*, *13*(8), 528–541. doi:10.1038/nrn3234

Rao, A., & Steward, O. (1993). Evaluation of RNAs Present in Synaptodendrosomes: Dendritic, Glial, and Neuronal Cell Body Contribution. *Journal of Neurochemistry*, *61*(3), 835–844. doi:10.1111/j.1471-4159.1993.tb03594.x

Rapier, C., Lunt, G. G., & Wonnacott, S. (1990). Nicotinic Modulation of [3H]Dopamine Release from Striatal Synaptosomes: Pharmacological Characterisation. *Journal of Neurochemistry*, *54*(3), 937–945. doi:10.1111/j.1471-4159.1990.tb02341.x

Richter, J. D. (2007). CPEB: a life in translation. *Trends in Biochemical Sciences*, *32*(6), 279–285. doi:10.1016/j.tibs.2007.04.004

Salmena, L., Poliseno, L., Tay, Y., Kats, L., & Pandolfi, P. P. (2011). A ceRNA Hypothesis: The Rosetta Stone of a Hidden RNA Language? *Cell*, *146*(3), 353–358. doi:10.1016/j.cell.2011.07.014

Salzman, J., Gawad, C., Wang, P. L., Lacayo, N., & Brown, P. O. (2012). Circular RNAs Are the Predominant Transcript Isoform from Hundreds of Human Genes in Diverse Cell Types. *PLoS ONE*, *7*(2), e30733. doi:10.1371/journal.pone.0030733

Sarkar, A., & Hochedlinger, K. (2013). The Sox Family of Transcription Factors: Versatile Regulators of Stem and Progenitor Cell Fate. *Cell Stem Cell*, *12*(1), 15–30. doi:10.1016/j.stem.2012.12.007

Schwanhäusser, B., Busse, D., Li, N., Dittmar, G., Schuchhardt, J., Wolf, J., et al. (2011). Global quantification of mammalian gene expression control. *Nature*, *473*(7347), 337–342. doi:10.1038/nature10098

Selbach, M., Schwanhäusser, B., Thierfelder, N., Fang, Z., Khanin, R., & Rajewsky, N. (2008). Widespread changes in protein synthesis induced by microRNAs. *Nature*, *455*(7209), 58–63. doi:10.1038/nature07228

Shapiro, J. A. (2009). Revisiting the Central Dogma in the 21st Century. *Annals of the New York Academy of Sciences*, *1178*(1), 6–28. doi:10.1111/j.1749-6632.2009.04990.x

Steward, O., & Levy, W. B. (1982). Preferential localization of polyribosomes under the base of dendritic spines in granule cells of the dentate gyrus. *The Journal of Neuroscience*, *2*(3), 284–291.

Steward, O., & Schuman, E. M. (2003). Compartmentalized Synthesis and Degradation of Proteins in Neurons. *Neuron*, *40*(2), 347–359. doi:10.1016/S0896-6273(03)00635-4

Sugino, K., Hempel, C. M., Miller, M. N., Hattox, A. M., Shapiro, P., Wu, C., et al. (2006). Molecular taxonomy of major neuronal classes in the adult mouse forebrain. *Nature Neuroscience*, *9*(1), 99–107. doi:10.1038/nn1618

Taylor, A. M., Dieterich, D. C., Ito, H. T., Kim, S. A., & Schuman, E. M. (2010). Microfluidic Local Perfusion Chambers for the Visualization and Manipulation of Synapses. *Neuron*, *66*(1), 57–68. doi:10.1016/j.neuron.2010.03.022

Tennyson, V. M. (1970). THE FINE STRUCTURE OF THE AXON AND GROWTH CONE OF THE DORSAL ROOT NEUROBLAST OF THE RABBIT EMBRYO. *The Journal of Cell Biology*, *44*(1), 62–79. doi:10.1083/jcb.44.1.62

Terrian, D. M., Johnston, D., Claiborne, B. J., Ansah-Yiadom, R., Strittmatter, W. J., & Rea, M. A. (1988). Glutamate and dynorphin release from a subcellular fraction enriched in hippocampal mossy fiber synaptosomes. *Brain Research Bulletin*, *21*(3), 343–351. doi:10.1016/0361-9230(88)90146-3

Thomas, M. G., Loschi, M., Desbats, M. A., & Boccaccio, G. L. (2011). RNA granules: the good, the bad and the ugly. *Cellular Signalling*, *23*(2), 324–334. doi:10.1016/j.cellsig.2010.08.011

Thorne, B., Wonnacott, S., & Dunkley, P. R. (1991). Isolation of Hippocampal Synaptosomes on Percoll Gradients: Cholinergic Markers and Ligand Binding Sites. *Journal of Neurochemistry*, *56*(2), 479–484. doi:10.1111/j.1471-4159.1991.tb08175.x

Timmusk, T., Palm, K., Metsis, M., Reintam, T., Paalme, V., Saarma, M., & Persson, H. (1993). Multiple promoters direct tissue-specific expression of the rat BDNF gene. *Neuron*, *10*(3), 475–489. doi:10.1016/0896-6273(93)90335-O

Tiruchinapalli, D. M., Oleynikov, Y., Kelic, S., Shenoy, S. M., Hartley, A., Stanton, P. K., et al. (2003). Activity-dependent trafficking and dynamic localization of zipcode binding protein 1 and beta-actin mRNA in dendrites and spines of hippocampal neurons. *The Journal of Neuroscience*, *23*(8), 3251–3261.

tom Dieck, S., Hanus, C., & Schuman, E. M. (2014). SnapShot: local protein translation in dendrites. [Neuron. 2014] - PubMed - NCBI. *Neuron*, *81*(4), 958–958.e1. doi:10.1016/j.neuron.2014.02.009

Ulitsky, I., Shkumatava, A., Jan, C. H., Sive, H., & Bartel, D. P. (2011). Conserved Function of lincRNAs in Vertebrate Embryonic Development despite Rapid Sequence Evolution. *Cell*, *147*(7), 1537–1550. doi:10.1016/j.cell.2011.11.055

Vandewalle, C., Van Roy, F., & Berx, G. (2009). The role of the ZEB family of transcription factors in development and disease. *Cellular and Molecular Life Sciences*, *66*(5), 773–787. doi:10.1007/s00018-008-8465-8

Vickers, C. A., Dickson, K. S., & Wyllie, D. (2005). Induction and maintenance of late-phase long-term potentiation in isolated dendrites of rat hippocampal CA1 pyramidal neurones. *The Journal of Physiology*, *568*(Pt 3), 803–813. doi: 10.1113/jphysiol.2005.092924

Vogel, C., & Marcotte, E. M. (2012). Insights into the regulation of protein abundance from proteomic and transcriptomic analyses. *Nature Reviews Genetics*, *13*(4), 227–232. doi:10.1038/nrg3185

Weiler, I. J., & Greenough, W. T. (1991). Potassium ion stimulation triggers protein translation in synaptoneurosomal polyribosomes. *Molecular and Cellular Neuroscience*, *2*(4), 305–314. doi:10.1016/1044-7431(91)90060-2

Whittaker, V. P., & Gray, E. G. (1962). The synapse: biology and morphology. *British Medical Bulletin*, *18*, 223–228.

Wilhelm, J. E., & Vale, R. D. (1993). RNA on the move: the mRNA localization pathway. *The Journal of Cell Biology*, *123*(2), 269–274. doi:10.1083/jcb.123.2.269

Witzmann, F. A., Arnold, R. J., Bai, F., Hrncirova, P., Kimpel, M. W., Mechref, Y. S., et al. (2005). A proteomic survey of rat cerebral cortical synaptosomes. *Proteomics*, *5*(8), 2177–2201. doi:10.1002/pmic.200401102

Zaphiropoulos. (2005). Circular RNAs. *Pnas*, 1–6.

Zhao, X., Tang, Z., Zhang, H., Atianjoh, F. E., Zhao, J.-Y., Liang, L., et al. (2013). A long noncoding RNA contributes to neuropathic pain by silencing Kcna2 in primary afferent neurons. *Nature Neuroscience*, *16*(8), 1024–1031. doi: 10.1038/nn.3438

Zhong, J., Zhang, T., & Bloch, L. M. (2006). Dendritic mRNAs encode diversified functionalities in hippocampal pyramidal neurons. *BMC Neuroscience*, *7*(1), 17. doi:10.1186/1471-2202-7-17

Zivraj, K. H., Tung, Y. C. L., Piper, M., Gumy, L., Fawcett, J. W., Yeo, G. S. H., & Holt, C. E. (2010). Subcellular profiling reveals distinct and developmentally regulated repertoire of growth cone mRNAs. *The Journal of Neuroscience*, *30*(46), 15464–15478. doi:10.1523/JNEUROSCI.1800-10.2010

CURRICULUM VITAE

For reasons of data protection, the curriculum vitae is not published in the electronic version.

For reasons of data protection, the curriculum vitae is not published in the electronic version.

August 2014 Berlin

Ana Babic

DECLARATION

The project was conceived and performed in the group of "Novel Sequencing Technology, Medical and Functional Genomics" in Berlin Institute for Medical Systems Biology at Max-Delbrück-Center for Molecular Medicine under the supervision of Dr. Wei Chen. I hereby declare that this thesis is the results of my own original research work. Contributions from others involved are clearly and specifically indicated in the acknowledgement. The thesis is submitted to Department of Biology, Chemistry and Pharmacy of Freie Universität Berlin to obtain the academic degree of Doctor rerum naturalium (Dr. rer. nat.) and has not been submitted to anywhere else for any degree.

August 2014 Berlin

Ana Babic